NASA CR-54545
PWA FR-1669

SINGLE STAGE EXPERIMENTAL EVALUATION OF SLOTTED ROTOR AND STATOR BLADING

PART II - ANNULAR CASCADE INVESTIGATION OF SLOT LOCATION AND GEOMETRY

PREPARED FOR
NATIONAL AERONAUTICS AND SPACE ADMINISTRATION
CONTRACT NAS3-7603
31 OCTOBER 1966

CONTRACTOR PROGRAM MANAGER: Charles G. Linder
CONTRACTOR PROGRAM ADVISOR: Burton A. Jones

TECHNICAL MANAGEMENT
NASA LEWIS RESEARCH CENTER
CLEVELAND, OHIO

NASA PROGRAM MANAGER: John E. McAulay
Air Breathing Engines Division
NASA RESEARCH ADVISOR: L. Joseph Herrig
Fluid Systems Components Division

Pratt & Whitney Aircraft
FLORIDA RESEARCH AND DEVELOPMENT CENTER
DIVISION OF UNITED AIRCRAFT CORPORATION
UA®

Printed in the United States of America

ABSTRACT

An annular cascade investigation was conducted to provide criteria for the design of slotted rotors and stators to be tested in a subsequent part of the overall program. The test stators were 65-series airfoils, having a chord length of 6.5 inches and a calculated midspan D-factor loading of 0.528 without slots. A slot located approximately midway between the point of minimum pressure and the point of separation produced the best performance, reducing the wake loss coefficient to about 17% of that for the unslotted vane and increasing the lift coefficient and air turning angle approximately 10% and 2 degrees, respectively.

Author

CONTENTS

ILLUSTRATIONS

ILLUSTRATIONS (Continued)

SECTION I
SUMMARY

An annular cascade investigation was conducted to provide criteria for the design of slotted rotors and stators to be tested in a subsequent part of the overall program. The test stators were 65-series airfoils, having a chord length of 6.5 inches and a calculated midspan D-factor loading of 0.528 without slots. The tests were conducted at an inlet Mach number of 0.64.

Initial tests of the unslotted stator disclosed that the minimum pressure and separation points occurred at 12 and 85% of the chord, respectively. Based on these data, two axial slot locations were selected. The forward location was at 55% of the chord on the suction surface, which was approximately halfway between the minimum pressure point and the flow separation point. The rearward point was selected at 75% of the chord, which was slightly ahead of the flow separation point for the unslotted configuration. In addition to slot location, several variations of slot geometry were tested at each slot location.

For the forward slot location, the stator wake loss coefficient varied between 17 and 43% of the unslotted loss coefficient, depending on the slot geometry utilized. For the rearward location, the loss coefficient ranged between 76 and 187% of the unslotted loss coefficient, depending on the slot geometry employed. Data for both slot locations indicated about the same increases in lift coefficient and air turning angle. The slot configuration with the lowest wake loss coefficient showed increases in lift coefficient and turning angle of about 10% and 2 degrees, respectively.

SECTION II
INTRODUCTION

Significant advancements in compressor technology require (1) advanced rotor and stator concepts in terms of improved blading for high flow Mach numbers, (2) high lift devices for stators and rotors, and (3) a more adjustable geometry to extend the stall-free flow range. Progress in any of these areas may result in a sizable reduction in the number of compressor stages required for any specific application, and an improved compressor.

Pratt & Whitney Aircraft is engaged in a program under NASA Contract NAS3-7603 to investigate the application of high lift devices (in the form of slots) to subsonic rotors and stators. A systematic investigation of slots will be made to establish the feasibility and extent to which slotted blade concepts can be used to increase allowable blade loadings and the stable operating range of compressor stages. To accomplish this objective, three stator blade rows and three rotor blade rows will be built and tested. Tests with stators will use a representative state-of-the-art rotor to generate the stator inlet flow.

A survey of the literature on slotted airfoils was conducted to determine if any design information applicable to compressor blading existed. A bibliography is presented in Appendix C. The results of this survey showed that, whereas much data exist for isolated airfoils at low Mach numbers, slot design criteria applicable to high speed cascades are not available. It was therefore proposed, as part of the contract design effort, to conduct a series of annular cascade tests with slotted stators to establish preliminary criteria for the design of the slotted rotors and stators for the rotating stage test program.

A set of high turning inlet guide vanes was used to establish the whirl distribution into the stator test blade row of the annular cascade. These guide vanes were designed to produce essentially a constant flow angle from hub to tip for the 0.8 hub-tip ratio test vehicle. The test stator had a constant section from root to tip and had no twist. Initial tests were conducted with the unslotted stator blades to obtain their pressure distribution and flow separation point. On the basis of these

tests, two chordwise slot locations were chosen, and a range of slot geometries was investigated for each location. Because of the preliminary nature of these tests, only mean radius data were obtained for essentially one flow condition, angle of attack, and Mach number. Selection of the best slot location and geometry was based on wake loss, integrated lift coefficient, and cascade turning. This report presents the details of the test equipment, procedures, and test results for this preliminary annular cascade study.

SECTION III
TEST EQUIPMENT

A. TEST FACILITY

The annular cascade tests were conducted in the compressor research facility shown in figures III-1 and III-2.* In the nonrotating mode of operation, a J75 engine is used in conjunction with a two-stage ejector system to draw ambient air through the compressor rig. Flow rates up to approximately 110 lb/sec are possible at atmospheric inlet pressure. Ambient air enters the compressor test rig through a 78-foot inlet duct, plenum chamber, and bellmouth inlet and exhausts through the ejector system. Airflow rate is measured by means of an ASME thin plate orifice located in the inlet duct. The plenum chamber is sufficiently large to provide essentially stagnation conditions upstream of the bellmouth inlet to the test rig, and a long diffuser ahead of the plenum ensures uniform conditions across the chamber.

The inlet duct and plenum chamber are mounted on a track and can be rolled away from the test rig. A pneumatic tube seal is used to prevent air leakage between the plenum chamber and test rig.

B. COMPRESSOR TEST RIG

The compressor test rig consisted of a bellmouth inlet, support struts, inlet guide vanes, test stators, and an exhaust diffuser section, as shown schematically in figure III-3. Inner and outer wall diameters at axial stations of interest are tabulated in the figure. The desired gas path was formed by fabricated wooden filler sections. A split test case provided convenient accessibility for blading changes without removing the entire rig from the test stand.

The test section had a hub/tip ratio of approximately 0.8, and was comprised of a row of 50 inlet guide vanes that set the stator inlet conditions and a row of 20 test stators that turned the flow back to the near-axial direction. The inlet guide vane and stator blade row assemblies were each divided into two 180-degree sections. The guide vanes were fabricated from stainless steel and tack-welded to the shrouds. The stator and stator

*Figures are presented in Appendix D.

shrouds were fabricated from aluminum and the stators were positioned with dowel pins and held in place with machine screws, as shown in figure III-4. For the slotted stator tests, only the vanes in the upper 180-degree section were slotted.

C. INLET GUIDE VANE DESIGN

The inlet guide vanes were designed for a constant turning of 50.4 degrees. NACA series 63 blade sections were chosen for this blade row. Details of this design are listed in table III-1.

D. STATOR DESIGN

Selection of the stator configuration for slot evaluation was based on the criterion that the stator should be typical of the blading geometry to be used in the rotating phase of the program. The 65-series airfoil section was selected for the stator vane profile (NACA 65-(16)09). A vane chord of 6.5 inches was chosen to permit the installation of sufficient static pressure instrumentation, and to provide a large scale model that would allow accurate determination of the effect of small changes in slot geometry.

The stator vane had a constant equivalent circular arc camber of 38.85 degrees from the hub to the tip and was untwisted. The loading (D-factor) distribution from hub to tip was 0.55 to 0.50 with a value of 0.528 at the mean radius. The inlet Mach number varied from 0.67 at the hub to 0.61 at the tip with a mean radius value of 0.637. Other details of the stator design are given in table III-1.

Table III-1. Summary of Design Data For The Inlet Guide Vane and Test Stator

	Inlet Guide Vane			Stator		
	Hub	Mean	Tip	Hub	Mean	Tip
Series Airfoil	63	63	63	65	65	65
Chord (in.)	3.00	3.00	3.00	6.546	6.546	6.546
Thickness Ratio	0.06	0.06	0.06	0.09	0.09	0.09
Camber (deg)*	-72.8	-72.8	-72.8	38.8	38.8	38.8
Inlet Metal Angle (deg)*	-18.2	-18.2	-18.2	48.9	48.9	48.9
Exit Metal Angle (deg)*	54.6	54.6	54.6	10.1	10.1	10.1
Aspect Ratio	1.306	1.306	1.306	0.554	0.554	0.554

*Based on equivalent circular arc meanline.

Table III-1. Summary of Design Data For The Inlet Guide Vane and Test Stator (Continued)

	Inlet Guide Vane			Stator		
	Hub	Mean	Tip	Hub	Mean	Tip
Blade Chord Angle (deg)	35.7	35.7	35.7	29.5	29.5	29.5
Solidity	1.412	1.294	1.200	1.234	1.237	1.054
Inlet Absolute Mach Number	0.321	0.321	0.321	0.674	0.637	0.6085
Inlet Absolute Air Angle (deg)	0.0	0.0	0.0	51.6	50.4	49.3
Exit Absolute Air Angle (deg)	51.6	50.4	49.3	22.7	21.7	21.9
Diffusion Factor				0.552	0.528	0.504
Loss Coefficient	0.139	0.139	0.139	0.0439	0.0382	0.0348
Deviation (deg)	3.0	4.2	5.3	12.6	11.6	11.8

E. INSTRUMENTATION

Instrumentation was provided primarily for the measurement of midspan wake profile, chordwise pressure distribution, and stator air turning. Axial location of instrumentation stations are shown in figure III-3, and schematics showing the instrumentation in detail are presented in figures III-5 to III-9. The two instrumentation stations of primary concern are Stations 2 and 3A. Station 2 was located just ahead of the test stators and Station 3A was about 1/2 chord length downstream of the stators.

1. Instrumentation for Rig Inlet Conditions

Weight flow was measured with an ASME standard thin plate orifice located in the inlet duct.

Six static pressure taps and six temperature probes were located in the plenum chamber for measurement of inlet total pressure and temperature. The circumferential and radial locations for this instrumentation are shown in figure III-6.

Three static pressure taps were located on both the inner and outer walls upstream of the inlet guide vanes (Station 0). From a rig calibration over a wide range of weight flows, a calibration between these static pressures and weight flow was derived and used to check subsequent weight flow measurements.

2. Stator Inlet; Station 2

Stator inlet conditions were measured at Station 2. A section view of the flow path at Station 2, showing the circumferential and radial location of the instrumentation, is presented in figure III-6. Inlet air angle measurements were obtained at three circumferential locations with 20-degree wedge traverse probes. Three Kiel probes were used for midspan total pressure measurement, and a wake probe was installed to measure inlet guide vane wake total pressure distribution. The wake probe was approximately aligned with the average guide vane exit air angle. Three static pressure taps were located on both the inner and outer wall.

A 20-degree wedge probe was added during the test program at midspan-midchannel approximately 1/2 chord length downstream of the inlet guide vane row (Station 1). This probe was added for measurement of guide vane exit angle at a position that was not influenced by the guide vane wakes. Figure III-6 shows the location of this probe in a section view of the flow path.

3. Stator Exit; Station 3A

Stator exit conditions were measured at Station 3A. A section view of the flow path at this station is shown in figure III-6.

Four 20-degree wedge traverse probes were used for stator exit angle measurement and four Kiel probes were used for midspan total pressure measurement. Two of the traverse probes were added during the test program. A wake probe was used for stator wake total pressure measurement. Eight static pressure taps were located around the outer wall to detect the presence of flow nonuniformity that might occur as a result of having unslotted stators in the lower half of the test section. Two static taps were located in the inner wall.

4. Stator Surface Pressure Taps

Three test stator vanes were instrumented with static pressure taps to provide a sufficient number of chordwise pressure measurements. The instrumented vanes are designated A, B, and C in figure III-5. The spanwise and

chordal locations of the pressure taps are shown in figure III-7. The location of taps in the slot region are shown in figures III-8 and III-9 for the forward and rear slots respectively. Figure III-10 illustrates the method of installation of the pressure taps.

Installation tolerances from vane to vane caused a small variation in stagger angle and consequently incidence angle. Because static pressure distribution is a function of incidence angle, stagger angles are tabulated below for the vanes with surface static pressure taps.

	Vane A γ°, deg	Vane B γ°, deg	Vane C γ°, deg
Unslotted and Forward Slot Configurations	29.0	29.75	30.0
Rear Slot Configurations	29.0	29.17	29.08

5. Description of Probes

Details of the 20-degree wedge probe, wake probe, and Kiel probe are shown in figure III-11. The wedge probe contained side pressure pickups for air angle measurement, a total pressure pickup, and a total temperature pickup.

The wake probe contained 16 total pressure pickups formed by 0.042-in. (OD) hypo tubing and spaced as shown in the figure.

6. Instrumentation Readout

All pressure and angle data were automatically recorded. Traverse probe data (total pressure and air angle) were recorded on magnetic tape at the rate of 60 samples (2.5 inches probe travel) per minute. Steady-state pressure measurements were obtained using Scannivalve multi-channel pressure transducer system that includes automatic data recording on IBM cards. Temperatures were indicated on a precision potentiometer, and manually recorded on IBM cards.

Plenum conditions and flow measuring orifice measurements were also recorded on manometer tubes in the test stand control room to permit setting the desired corrected flow conditions.

SECTION IV
PROCEDURES

A. TEST PROCEDURE

Two tests were conducted with the unslotted stators to provide data on which to base slot location and to provide data for a comparison between the unslotted and slotted stator performance. Subsequent tests involved alternative use of a forward and rear slot configuration. To simplify testing, it was desirable to slot only the stator vanes in the upper half of the annulus. Comparisons of circumferential distributions of wall static pressure for the unslotted tests and the initial slotted tests indicated that although there was a definite circumferential variation of static pressure, the pattern did not change appreciably when slotted vanes were installed in only the upper half of the annulus. Therefore, it was considered adequate to slot only half of the test vanes for this preliminary slot configuration investigation. A comparison of wall static pressures at the stator exit with and without slotted stators in the upper half of the test section is shown in figures IV-1 and IV-2.

The tests were conducted at an approximate stator inlet Mach number of 0.64 and a corresponding corrected weight flow of 81.5 lb/sec. Flow conditions were set by controlling the J75 slave engine exhaust flow through the ejector system. When steady-state flow conditions were established, fixed instrumentation pressure and temperature measurements were recorded. The traverse probes were then actuated and data recorded, followed by a second recording of fixed instrumentation pressures and temperatures.

Immediately before the end of each test, a solution of Blue Dykem metal marking dye and alcohol was injected through static pressure orifices onto the suction and pressure surfaces of the three instrumented stator vanes to provide visual inspection of the boundary layer flow characteristics.

B. DATA REDUCTION PROCEDURE

1. Preliminary Data Reduction

An IBM computer program was used to convert magnetic-tape-recorded data and data recorded on IBM cards to engineering units. Traverse data (total pressure, total temperature, and air angle), obtained at approximately 0.04-inch increments across the span, were automatically plotted (as well as tabulated). The tabulated data were used to select midspan values of total pressure and air angle. The plotted data were inspected for general profile shape, as well as for inlet guide vane wake and secondary flow influences.

2. Parameter Calculation

The following parameters were calculated for the analysis of test data and the evaluation of slotted stator performance. Symbols are defined in Appendix A.

a. Static Pressure Coefficient

Stator vane surface static pressure measurements are presented in the form of pressure coefficients, defined as follows:

$$C_P = (p_\ell - \overline{P}_2)/\overline{q}_2$$

where:

p_ℓ = local vane surface pressure

$\overline{P}_2$ = arithmetic average of wall static pressures upstream of stator (Station 2)

$\overline{q}_2 = \frac{\gamma}{2}\overline{P}_2 M_2^2$

$\gamma = 1.40$

$M_2 = f\left[\overline{P}_2/\overline{P}_2\right]$

and

$\overline{P}_2$ = area-average total pressure at Station 2 (midspan)

b. Total Pressure Loss Coefficient

Total pressure loss coefficient for the inlet guide vanes is defined as

$$\bar{\omega}_{0-2} = \frac{\bar{P}_0 - \bar{P}_2}{q_0}$$

Guide vane inlet dynamic pressure, q_0 was obtained as a function of inlet Mach number, M_0, which was determined from isentropic flow relationships using measured weight flow, plenum pressure and temperature, and the appropriate flow area.

Stator vane wake total pressure loss coefficient is defined as

$$\bar{\omega}_{2-3A} = \frac{\bar{P}_2 - \bar{P}_{3A}}{\bar{q}_2}$$

where $\bar{P}_{3A}$ is the area-average total pressure at Station 3A (stator exit). Area-average total pressure at Stations 2 and 3A were obtained by manual integration of midspan wake total pressure distributions.

c. Total Pressure Loss Parameter

Wake total pressure loss is also presented in terms of the loss parameter

$$\frac{\bar{\omega}_{2-3A} \cos \beta_{3A}}{2\sigma}$$

where:

β_{3A} = stator exit air angle (Station 3A)
σ = solidity, ratio of chord to spacing

d. Diffusion Factor

Diffusion factor is defined as

$$D_F = 1 - \frac{V_{3A}}{V_2} + \frac{\Delta V_{\theta\ 2-3A}}{2\sigma V_2}$$

where:

V_2 = velocity at inlet to stator (Station 2)

V_{3A} = velocity at exit of stator (Station 3A)

and

$\Delta V_{\theta\ 2\text{-}3A}$ = change in tangential velocity across the stator

e. Lift Coefficient

Lift coefficient is defined as

$$C_L = \frac{\int (p_p - p_s)dc}{\bar{q}_2 c}$$

where:

p_p = static pressure on pressure surface

p_s = static pressure on suction surface

c = stator vane chord length

The pressure area term, $(p_p - p_s)dc$, was obtained by manual integration of the static pressure distributions. Each section of the slotted stator vanes was treated as a separate airfoil for the integration.

f. Stator Air Turning

Because of the influence of inlet guide vane wakes and secondary flows, the air angle measurements at midspan for different probes at a particular station varied by several degrees. The evaluation of the effect of slots on turning angle was therefore based on a study of individual probes selected on the basis of their proximity to wakes and the uniformity of indicated pressure and angle profiles in the midspan region.

SECTION V
RESULTS AND DISCUSSION

As stated previously, the objective of the annular cascade investigation of slotted stators was to provide guidelines for the design of slotted rotors and stators to be tested in a subsequent part of the overall program. In accordance with this objective, the cascade program was limited to the evaluation, based on mean radius measurements, of eleven slot geometry configurations and two slot locations. No attempt was made to resolve circumferential variations in wall static pressure and air angle; and end-wall boundary layer development through the 6.5-inch chord cascade was ignored.

The results of the annular cascade tests are presented in this section. Tabulations of total pressure, static pressure, and air angle data are included in Appendix B.

A. UNSLOTTED STATOR VANE PERFORMANCE

1. Inlet Guide Vanes

a. Exit Air Angle

Midspan air angle measurements behind the inlet guide vanes are summarized in table B-1. Air angle measurements obtained with each of the four wedge traverse probes are generally within ± 1.0 degree of the average angle for each probe. The air angles for different probes range from 45.3 to 53.7 degrees. This variation is attributed to slight differences in the location of each probe relative to adjacent guide vane wakes. On the basis of their overall average value, the guide vane exit air angles indicate that the stator may have been operating at approximately 2 degrees below design incidence, which would slightly unload the stator. Since the midspan air angle measurements encompassed the design value of 50.4 degrees, no attempt was made to improve the data by relocating probes to eliminate possible guide vane wake influence. Also, it was not considered necessary within the scope of the annular cascade program to restagger the guide vanes to increase the average exit angle to the design value. The guide vane design exit air angle was subsequently used in conjunction with stator exit air angles for evaluation of stator turning.

A typical measured spanwise distribution of air angle is compared with the design air angle distribution in figure V-1. The slope of the measured angle distribution matches that of the design distribution fairly well between about 25 and 75% span at a level approximately 2 degrees below the design values.

b. Total Pressure Loss

A typical guide vane midspan wake total pressure profile is shown in figure V-2. The profile is plotted as the ratio of local total pressure to inlet guide vane total pressure, P/P_0, vs channel distance in the plane of the probe. Vertical lines in the figure indicate the mid-channel projections of two adjacent channels. The wake probe was positioned so that it overlapped one complete channel width.

The size of the wake, with respect to the channel width, appears large because the measuring station is about 2 chord lengths downstream of the guide vane exit plane. The maximum local total pressure deficiency in the wake is very small (approximately 2%). The range of integrated values of total pressure ratio, $\overline{P}_2/P_0$, for all but two of the tests varied between 0.9953 and 0.9959. An average value of 0.9956 was used for all of the stator total pressure loss coefficient calculations. The guide vane loss coefficient based on this average total pressure ratio and an inlet Mach number of 0.324 is 0.0643, compared with the design loss coefficient value of 0.139.

2. Stators

a. Pressure Coefficient Distribution

The pressure coefficient (C_p) curve for the unslotted stator (Configuration 1) is presented in figure V-3. Table B-2 lists the pressure coefficients for two different unslotted stator tests (Configurations 1 and 1A). Note in figure V-3 that the pressure coefficient curve flattens out at approximately 85% chord on the suction surface; this indicates apparent flow separation at this point. This is supported by the dye patterns shown in figure V-4, which indicate flow separation at approximately the same chordal location.

The suction surface portion of the curve in figure V-3 was drawn through the Vane A pressure coefficient data to permit consistent comparisons with the forward and rear slot configuration pressure coefficient distributions, as discussed in Section V, paragraph C.2.

b. Total Pressure Loss

Midspan wake total pressure profiles for the two unslotted stator configuration tests are shown in figure V-5. Total pressure data are presented in table B-3. Values of loss coefficient, $\bar{\omega}$, based on integration of the wake profiles shown in figure V-5, are 0.071 and 0.068 for Configurations 1 and 1A, respectively.

Value of midspan loss parameter, $\frac{\bar{\omega}\cos\beta}{2\sigma}$, and D-factor for the unslotted stators were calculated for comparison with NACA stator loss data published in Reference 1*. The calculated values are listed as follows:

Configuration	1	1A
Loss parameter	0.029	0.028
D-Factor	0.442	0.466

These results are compared in figure V-6 with NASA stator mean radius loss data for NACA 65-A_{10} series airfoils and a loss correlation curve that represents root, mean, and tip section loss measurements for the NACA 65-A_{10} series and double circular arc airfoils. Although the two annular cascade test points are not in good agreement with the correlation curve, they correlate fairly well with the NASA stator mean radius data.

c. Air Turning Angle

Midspan stator exit air angles for the two unslotted stator tests are listed below:

Probe Circumferential Location, deg	24	228
	Stator Exit Air Angle, deg	
Configuration 1	23.8	21.4
Configuration 1A	23.7	21.4

The difference in the air angle values for the two different probes is attributed partly to their relative proximity to the adjacent stator vane wake. The probe at circumferential position 24 degrees is in close proximity to a vane pressure surface, whereas the probe at 228 degrees

*Reference 1: Aerodynamic Design of Axial Flow Compressors (Revised), NASA SP-36, 1965, pp 240 and 248.

is in close proximity to a vane suction surface. The angle measurements obtained with the first probe are therefore considered more reliable than those of the second probe. Based on the guide vane design exit angle of 50.4 degrees and the stator exit angles obtained with the 24-degree probe, the unslotted stator turning was 26.6 degrees compared with a design stator turning of 28.7 degrees.

B. SLOT CONFIGURATION SELECTION

1. Slot Location

The following general criteria were established to determine the location of slots for the stator vanes:

1. The slot should be located upstream of the point of flow separation. If the slot flow exhausted into a separated region, it could not effectively turn the primary flow back toward the suction surface.

2. The slot should be located in a region where the pressure difference between the suction and pressure surfaces is sufficiently high to provide high slot flow velocity. High slot flow velocity was considered important in permitting sufficient energy addition to the suction surface boundary layer to provide unseparated flow essentially to the blade trailing edge.

The pressure coefficient distribution in figure V-3 indicates suction surface boundary layer separation at about 85% chord and a maximum pressure difference across the vane at approximately 12% chord (minimum pressure point location on suction surface). On the basis of the general criteria above, two slot locations between 12 and 85% chord were selected for evaluation. One slot was located at 75% chord, close to the separation point. The slot flow at this location was expected to eliminate flow separation by energizing the boundary layer region. The second slot was located at 55% chord. The function of the slot flow at this location was to energize the boundary layer prior to incipient separation.

2. Slot Geometry

Slot geometry variables of primary concern in this investigation were slot contraction ratio, Y_1/Y_2; Coanda radius, R; and pressure surface leading edge radius, r_1. Definitions of the geometry nomenclature and a summary of the slot dimensions for all of the configurations is presented in figure V-7. Although slot angle, ψ, and pressure surface radius, R_p, are considered to be significant variables, they were not systematically evaluated in this investigation.

The slot exit width, Y_2, was calculated on the basis of an arbitrary slot flow requirement equal to approximately 3% of the primary flow, using the theoretical pressure drop between the pressure and suction surfaces. The resulting slot configurations are shown in figures V-8 and V-9 for the forward and rear slots, respectively. Configurations not indicated in the sequence of configuration numbers between 2 and 18 refer to test geometries and Reynolds number conditions that were omitted from the planned test program as warranted on the basis of test results.

C. SLOTTED STATOR VANE PERFORMANCE

1. Total Pressure Loss

Midspan total pressure data for the slotted stator configurations are summarized in table B-3. Wake profiles for a forward slot and a rear slot stator configuration are compared with an unslotted vane wake profile in figures V-10 and V-11, respectively. Midspan wedge and Kiel probe readings were translated to the wake probe channel and are superimposed on the wake profile for comparison. The actual circumferential locations of these probes are indicated in degrees.

Figure V-10 shows a comparison of an unslotted vane wake with the wake obtained with forward slot configuration 9. A significant reduction in wake size can be seen with a shift of the wake toward higher flow turning. The slight dip in pressure at channel distances of 0.6 and 2.0 inches are attributed to inlet guide vane wakes. A third guide vane wake appears at 3.6 inches where the stator vane wake is reduced because of the slot. In general, excellent agreement is seen between the translated probe pressures and the wake

probe pressures. The mismatch of the two Kiel probe readings in figure V-10 is attributed to their respective proximity to the steep part of the wake.

The wake profile for rear slot configuration 4 is compared with an unslotted vane wake profile in figure V-11. The rear slot wake is similar in size to that of the unslotted stator vane; however, a noticeable shift of the wake toward higher turning is apparent.

Midspan values of loss parameter and D-factor calculated for the slotted stator configurations are compared in figure V-12 with the NASA stator loss data (Reference 1). The annular cascade unslotted stator results are included for comparison. Loss coefficient, loss parameter, and D-factor for all of the annular cascade stator test configurations are summarized in table V-1.

Table V-1. Loss Coefficient, Loss Parameter, and D-Factor for Annular Cascade Stator Test Configurations

Configuration	D-Factor	$\bar{\omega}_{2\text{-}3A}$	$\frac{\bar{\omega}_{2\text{-}3A}\cos\beta_{3A}}{2\sigma}$
Unslotted			
1	0.442	0.071	0.029
1A	0.466	0.068	0.028
Slot at 55% Chord			
2	0.429	0.028	0.012
5	0.437	0.021	0.009
7	0.460	0.031	0.013
9	0.458	0.012	0.005
15	0.439	0.014	0.006
18	0.456	0.030	0.013
Slot at 75% Chord			
4	0.487	0.063	0.039
6	0.476	0.053	0.022
8	0.476	0.073	0.030
10	0.512	0.130	0.055
14	0.531	0.125	0.054

The 55% chord slot data in figure V-12 show a significant reduction in loss parameter level at the same general loading level as the unslotted stators. Also, a significant improvement in loss is indicated when compared to the NASA loss correlation curve and the NASA midspan stator loss data for 65-A_{10} series airfoils. The losses and D-factor values for the 75% chord slot configurations are generally higher than those for the unslotted stator and NASA data. It was apparent from the wake profile in figure V-11 that the rear slot location had little effect on the size and shape of the stator wake, although the wake was shifted about 2 degrees toward higher turning. The higher D-factor level obtained with the rearward slot as compared to the unslotted configuration may be attributed to three-dimensional effects.

It is apparent from inspection of the D-factor values for all of the stator configurations that the slots did not affect turning sufficiently to produce a significant improvement in loading. It is considered that secondary flow build-up at the endwalls through the relatively long chord stator limited the loading level capability of both slotted and unslotted stators.

2. Lift Characteristics

Stator vane static pressure distributions were manually integrated according to the method discussed in Section IV, Paragraph B.2, to obtain lift coefficient. Static pressure data, in the form of pressure coefficients, are presented in table B-2. Pressure coefficient distributions for a typical forward slot configuration (9) and a typical rear slot configuration (4) are shown in figures V-13 and V-14, respectively. The pressure measurements obtained on stator vanes A, B, and C (figure III-5) are indicated by symbol. The difference in suction surface pressure coefficients for vane A and vane B in figure V-13 is believed to have resulted from the approximately 1.0-degree difference in stagger angle for these two vanes, as discussed in Section III, Paragraph E.4. The curves drawn through the data points in figure V-13 favor the vane A data because the installed chordal stagger of vane A most nearly matches the installed chordal stagger angles of vanes A and C for the rear slot configurations. The suction surface pressure coefficients for vanes A and C for the rear slot configuration in figure V-14 are seen to be in close agreement.

Although the pressure taps exposed in the slot regions of the three instrumented vanes were not all perpendicular to the surface, the pressures indicated by these taps were used as guides in defining the pressure distribution for the two separate airfoil sections. Dashed portions of the curves indicate where the distribution shape was estimated for integration purposes.

It is worth noting that the level of pressure on the suction surface at the forward slot exit is considerably lower (C_p = -1.0) than the level of pressure at the rear slot exit (C_p = -0.3). The relatively high velocity associated with the lower of the two pressures is a necessary part of the desired Coanda effect at the slot exit.

Lift coefficients for all of the stator configurations are shown in table V-2. In general, both the forward and rear slot configurations appear to have produced a slight increase in lift coefficient over that of the unslotted stator. The pressure data scatter negates a more detailed evaluation of lift coefficient.

Table V-2. Lift Coefficients for Stator Configurations

Configuration	Lift Coefficient
Unslotted	
1	0.710
1A	0.680
Forward Slot	
2	0.665
5	0.716
7	0.762
9	0.768
15	0.716
18	0.707
Rear Slot	
4	0.765
6	0.732
8	0.744
10	0.661
14	0.705

3. Air Turning Angle

Stator exit air angles are summarized in table B-5. Angle measurements obtained with probes at circumferential locations of 24, 65, 228, and 328 degrees are presented. The probe located at 228 degrees was in the lower half of the annulus behind unslotted stator vanes. Air angles obtained with the probe at 24 degrees were selected for comparison with the unslotted stator exit air angles because of the lack of sufficient comparative data at the other circumferential location behind the slotted vanes. A typical air angle distribution obtained with this probe is shown in figure V-15. The measured mean radius air angle and the design air angle distribution for the unslotted stator are included in the figure for comparison. The unslotted stator exit air angle (Section V, Paragraph A.1) was 23.8 degrees. The average stator exit air angle is 22.0 degrees for the forward slot configurations and 21.4 degrees for the rear slot configurations, resulting in an average increase in turning of about 2 degrees due to slots. This level of turning increase is generally consistent with the increase in lift coefficient that resulted from the slots. As shown in table B-5, no consistent variation in air turning was indicated for the slot configurations tested.

SECTION VI
CONCLUDING REMARKS

Eleven slotted stator configurations and two slot chord locations were evaluated in an annular cascade of 6.5-inch chord stators to provide slot design guidelines for single stage rig blading. The relative performance characteristics of the different configurations were evaluated on the basis of loss coefficient, D-factor loading, lift coefficient, and turning calculated from mean-radius measurements. Although this investigation was limited in scope, it was extremely valuable in supplying the information needed to develop preliminary slot design criteria for application to the single stage rotor and stator blading that will be tested in a subsequent part of the overall program. A preferred slot location at approximately half the distance between the minimum pressure point and the separation point was determined. This slot location provided a greater reduction in wake loss than that obtained with a slot located in close proximity to the separation point. A preferred slot geometry was determined on the basis of minimum wake loss and maximum lift coefficient.

A. EFFECT OF SLOT LOCATION ON PERFORMANCE

Although both slot locations produced an increase in exit air angle and lift coefficient, the slot at 55% chord produced a considerably greater reduction in wake loss than the slot at 75% chord. This result is attributed to two factors:

1. The available pressure drop across the stator vane (pressure-to-suction surface) at the 75% chord slot location was less than the pressure drop across the vane at the 55% chord slot location.

2. The suction surface boundary layer at 75% chord is thicker than at 55% chord.

The first of the above factors results in a relatively low slot flow velocity and thus reduces the Coanda effect. The thicker boundary layer requires a larger pressure gradient normal to the suction surface

to induce freestream flow toward the surface. These factors tend to support the result that the rear slot wake was shifted toward higher turning but not reduced in size (figure V-11).

B. EFFECT OF SLOT GEOMETRY ON PERFORMANCE

The effect of slot geometry on performance was less pronounced than the effect of slot location. The geometry parameter that produced the most significant reduction in wake size for a forward slot configuration was the rear section leading edge radius, r_1, (figure V-7). When this radius was increased from 0.028 to 0.056 in., the wake loss coefficient decreased from 0.031 to 0.012.

The Coanda radius was the most significant geometry parameter that was varied for the rear slot configuration. A slight increase in Coanda radius produced a slight decrease in wake loss (0.063 to 0.053). Subsequent increase in Coanda radius resulted in a large increase in wake loss coefficient (up to 0.130). This change in wake loss suggests the probability of an optimum Coanda radius. Insufficient data were obtained to evaluate the optimum Coanda radius for the forward slot location.

Additional two-dimensional or annular cascade investigation is needed to provide basic information on the mechanism of slot effectiveness. Such investigation should include systematic evaluation of slot location and geometry over a range of Mach numbers, incidence angles, and loading levels.

APPENDIX A
LIST OF SYMBOLS

Symbol	Description	Units
c	Chord length	in.
C_L	Lift coefficient	
C_p	Static pressure coefficient	
M	Mach number	
p	Static pressure	psia
P	Total pressure	psia
q	Dynamic pressure, $1/2\rho V^2$	psia
s	Blade spacing	in.
V	Velocity	ft/sec
β	Air angle, measured from axial line	deg
γ	Ratio of specific heats	
γ°	Blade chord angle	deg
σ	Solidity	c/s
$\bar{\omega}$	Total pressure loss coefficient	

Subscripts

ℓ	Local vane surface point
p	Pressure surface
s	Suction surface
θ	Tangential
0	Guide vane inlet station
1	Guide vane exit station
2	Stator inlet station
3A	Stator exit station

APPENDIX B
TABULATED DATA

Mean radius and wall static pressure data for all of the test configurations are presented in this appendix. The following tabulations are included:

Table B-1. Guide Vane Exit Air Angle

Configuration	Guide Vane Exit Air Angle (Midspan) β, deg			
	Station			
	1	2		
	Circumferential Location, deg			
	18	143	243	323
Unslotted				
1		46.9	51.8	48.0
1A		47.4	51.8	47.9
Forward Slot				
2		42.5	52.3	47.4
5		45.4	51.5	48.5
7		45.4	51.4	50.0
9		45.9	51.7	47.5
15	48.3	45.8	53.7	47.4
18	50.1		49.4	47.6
Rear Slot				
4		46.0	51.3	47.3
6		45.6	50.6	48.5
8		45.8	51.0	48.9
10	48.2	46.3	51.8	47.1
14	46.4	45.3	51.4	46.8

Table B-2. Static Pressure Coefficients

	Percent Chord	Percent Span	Unslotted Stator 1	Unslotted Stator 1A	Forward Slot Configurations 2	5	7	9	15	18	Rear Slot Configurations 4	6	8	10	14
Vane A	5	67.96	-0.6899	-0.6498	-0.5809	-0.7059	-0.8334	-0.9033	-0.6326	-0.8659	--	-0.6000	-0.7279	-0.5362	-0.5797
	10	50.00	-0.7562	-0.7046	-0.6625	-0.6866	-0.7831	-0.8447	-0.6212	-0.8114	-0.8157	-0.7881	-0.9038	-0.6743	-0.7623
	15	32.04	-0.7180	-0.7004	--	--	--	--	--	--	--	--	--	0.2171	0.2316
	20	58.98	-0.6879	-0.6159	-0.6421	-0.7138	-0.7869	-0.7980	-0.6415	-0.7142	--	-0.6975	-0.8702	-0.6502	-0.6845
	25	41.02	-0.6556	-0.6184	-0.5257	-0.5967	-0.5350	-0.6072	-0.5101	--	--	-0.6019	-0.7522	-0.5892	-0.5801
	30	67.96	--	--	-0.4957	-0.5649	--	-0.3418	--	--	--	-0.5400	-0.6721	-0.5006	-0.4699
Suction	35	50.00	--	--	-0.3934	-0.5541	-0.5534	-0.5112	-0.3345	-0.4927	--	-0.5409	-0.6423	-0.4263	-0.4256
Surface	40	32.04	-0.4781	-0.4608	-0.3207	-0.4502	--	-0.1309	-0.0212	--	-0.4881	--	-0.5542	-0.4022	-0.3797
	45	58.98	--	--	-0.2000	-0.3033	--	-0.0016	--	--	--	-0.3025	-0.4558	-0.2743	-0.2165
	50	41.02	-0.3471	-0.3657	0.1049	0.3095	0.4384	0.5621	0.5991	--	--	-0.2681	-0.4173	-0.2327	-0.2158
	55	67.96	--	--	-0.2553	-0.2708	-0.4616	-0.4273	-0.0449	-0.1798	-0.1529	-0.1434	-0.2663	-0.0667	-0.0801
	60	50.00	-0.1392	-0.1537	-0.6849	-0.8626	-1.0425	-1.0115	-0.5462	-0.7543	-0.1202	-0.0478	-0.1904	-0.0429	-0.0655
	65	32.04	-0.1062	-0.0025	-0.2059	--	-0.3394	-0.3155	-0.1370	-0.2991	-0.0189	-0.0022	-0.0843	-0.0241	0.0079
	70	58.98	--	--	-0.0148	--	--	-0.1783	-0.0323	-0.1259	--	--	--	--	--
	75	41.02	0.1108	0.0774	-0.0079	-0.0692	-0.1244	-0.1023	0.0358	-0.0530	--	--	--	--	--
	80	67.96	--	--	0.1411	0.0502	-0.0100	-0.0072	0.1076	0.0470	--	-0.3084	-0.4410	-0.1737	-0.0937
	85	50.00	0.2271	0.2102	0.1168	0.0443	0.0381	0.0572	0.1092	0.0760	-0.0378	0.0	-0.1173	-0.0371	-0.0718
	90	32.04	--	--	0.1368	0.1249	0.1356	0.1220	0.2006	0.1385	0.0622	0.0109	-0.5154	0.0486	0.0285
	95	67.96	--	--	0.1740	0.1393	0.1631	0.1743	0.2025	0.1811	0.1522	0.1631	-0.6170	0.1311	--
Vane C	2.5	67.96	-0.5310	-0.5587	-0.4872	-0.6026	-0.5972	-0.5095	-0.4991	-0.4653	-0.6135	-0.6375	-0.5596	-0.3737	--
	7.5	50.00	--	--	-0.6582	-0.7344	-0.6569	-0.5803	--	--	--	-0.7472	-0.6215	-0.6394	--
	12.5	32.04	-0.6984	-0.6413	-0.6079	--	-0.6894	-0.6102	-0.6851	-0.6391	-0.7869	-0.7547	-0.6359	-0.6286	--
	17.5	58.96	-0.7000	-0.6406	-0.6036	-0.7266	-0.7247	-0.6474	-0.7500	-0.6685	-0.7667	-0.7503	-0.8833	-0.6568	--
	22.5	41.02	-0.6327	-0.5629	-0.4924	-0.6039	-0.5778	-0.5105	-0.6028	-0.5224	-0.6849	-0.6138	-0.8000	-0.5781	--
	27.5	67.96	-0.5601	-0.5071	-0.3773	-0.5170	-0.4953	-0.4313	-0.5706	-0.4760	--	-0.5678	-0.7141	-0.5521	--
	32.5	50.00	--	--	-0.2924	-0.4370	-0.3991	--	-0.4456	-0.3915	--	-0.4928	-0.6439	-0.4921	-0.4785
Suction	37.5	32.04	-0.3993	-0.3675	-0.2069	--	-0.3372	-0.2720	-0.3978	-0.3129	--	-0.3988	-0.5391	-0.4130	--
Surface	42.5	58.98	-0.3477	-0.3216	-0.1046	-0.1977	-0.1772	--	-0.2576	-0.1612	-0.3333	-0.3131	-0.4647	-0.3187	--
	47.5	41.02	-0.1386	-0.1265	0.0595	-0.0679	-0.0525	--	-0.1307	-0.0666	-0.2750	-0.2409	-1.0490	-0.2879	--
	52.5	67.96	--	--	0.1654	--	0.2734	0.3632	0.5117	0.2666	-0.1628	-0.1531	-0.2833	-0.1702	--
	57.5	50.00	-0.0974	-0.0693	-0.7862	-1.0570	-0.9459	-0.8523	-0.8003	-0.4192	-0.0955	-0.0778	-0.2042	-0.1314	-0.1196
	62.5	32.04	-0.0245	-0.0018	-0.0069	-0.0839	-0.2819	-0.1816	-0.2259	-0.4057	-0.0013	-0.0028	-0.1138	-0.0438	--
	67.5	58.98	0.1016	0.0933	-0.0158	-0.0839	-0.0241	0.0188	-0.0266	-0.0356	--	--	--	--	-0.2918
	72.5	41.02	0.1399	0.1438	0.1513	-0.0285	0.0309	0.0645	0.0301	0.0644	--	--	--	--	-0.2003
	77.5	67.96	0.1908	0.1731	0.1526	0.1026	0.1575	0.1924	0.1263	0.1830	--	-0.3931	-0.5304	0.0057	-0.1142
	82.5	50.00	0.2082	0.2049	0.1993	0.1170	0.1472	0.1868	0.1256	0.1729	0.0407	0.0256	-0.0718	-0.1232	-0.0725
	87.5	32.04	0.2271	0.2053	0.1809	--	0.1528	0.1911	0.1497	0.1767	--	0.1316	0.0183	0.0810	0.0421
	92.5	67.96	0.2239	0.2230	--	--	0.4031	0.2516	0.2130	0.2035	0.7913	0.2206	0.1192	0.1784	0.1715
Vane B	0	32.04	1.0696	1.0378	1.0378	0.9928	1.0084	1.0520	1.0411	--	1.0561	1.0184	0.9670	1.0410	--
	5	50.00	0.3369	0.3287	0.1724	0.5020	1.1847	0.1714	0.1446	0.0789	0.2785	0.2556	0.1234	0.2317	0.0789
	10	67.96	0.3693	0.3498	0.2398	0.2195	0.1428	0.2398	0.2348	0.1631	0.2947	0.2981	0.1990	0.2854	0.1631
	15	41.02	0.3498	0.3393	0.1694	0.1868	0.1188	0.2099	0.2003	0.1473	0.3140	0.1990	0.2237	0.2746	0.1473
	20	58.98	0.3716	0.3604	0.2563	0.2003	0.1881	0.2263	0.2652	--	0.3301	0.3166	0.2138	0.3216	--
	25	32.04	0.3578	0.3318	0.2000	0.1538	--	--	--	--	0.3109	0.2697	0.1974	0.3105	--
	30	50.00	0.3794	0.3622	0.1931	--	--	--	--	--	0.3407	0.3269	0.2378	0.3375	--
Pressure	35	67.96	0.3967	0.3693	--	--	0.3456	--	0.4652	0.3609	0.3603	0.3319	0.2577	0.3381	0.3609
Surface	40	41.02	0.3977	0.3671	0.3365	0.3613	0.4184	0.4849	0.4788	0.3959	0.3429	0.3159	0.2433	0.3241	0.3959
	45	58.98	0.4065	0.3717	0.2510	0.1997	0.5059	0.5447	0.5937	0.5120	0.3465	0.3356	0.2510	0.3295	0.5120
	50	32.04	--	--	0.4914	0.4413	0.3950	0.4411	0.4161	--	--	0.3013	0.6817	0.2962	--
	55	50.00	0.4356	0.4163	0.4888	0.4216	0.4234	0.4707	0.4608	0.3953	--	--	0.7208	--	0.3953
	60	67.96	0.4716	0.4544	0.5069	--	0.5284	0.4928	0.4797	0.4394	--	0.4247	0.3353	0.4016	0.4394
	65	41.02	0.4859	0.4661	0.5178	0.4908	0.4675	0.5016	0.5146	0.4533	--	--	0.3151	--	0.4533
	70	58.98	0.5144	0.5053	0.5428	--	0.4988	0.5342	0.5367	0.5013	--	--	0.3208	--	0.5013
	75	32.04	0.5284	0.5251	0.5526	0.5056	0.5016	0.5375	0.5335	0.5003	--	--	--	--	0.5003
	80	50.00	0.5389	0.5396	0.5684	--	0.5219	0.5523	0.5604	--	0.6577	0.6415	0.5756	--	--
	85	67.96	0.5359	0.5230	0.5842	0.5370	0.5184	0.5438	0.5415	0.5243	--	0.6175	0.5439	0.6092	0.5243
	90	58.98	--	--	0.5875	0.5501	--	0.5553	0.5703	0.5423	0.6356	0.6219	0.5644	0.6232	0.5423

Table B-3. Total Pressure, Midspan (psia)

Configuration		1	1A	2	5	7	9	15	18	4	6	8	10	14
Plenum Pressure, P_o		14.391	14.413	14.376	14.416	14.368	14.407	14.424	14.466	14.449	14.466	14.393	14.380	14.430
Probe	Circumferential Location, deg							Station 2 (Stator Inlet)						
Wake Probe	114.0													
	1 (Tube No.)			14.359	14.387	14.410	14.380	14.393	14.429	14.357	14.435	14.373	14.366	14.429
	2			14.374	14.416	14.425	14.408	14.422	14.443	14.429	14.464	14.388	14.381	14.429
	3			14.374	14.416	14.438	14.408	14.422	14.443	14.429	14.464	14.388	14.381	14.429
	4			14.359	14.416	14.410	14.408	14.422	14.443	14.429	14.464	14.388	14.381	14.429
	5			14.374	14.416	14.424	14.408	14.422	14.443	14.443	14.464	14.388	14.381	14.429
	6			14.374	14.416	14.417	14.408	14.235	14.443	14.443	14.464	14.388	14.381	14.429
	7			14.374	14.387	14.396	14.394	14.393	14.443	14.429	14.449	14.373	14.381	14.415
	8			14.259	14.344	14.281	14.322	14.307	14.356	14.371	14.377	14.287	14.349	14.357
	9			14.087	14.171	14.094	14.136	14.105	14.154	14.227	14.218	14.085	14.093	14.169
	10			14.087	14.127	14.152	14.351	14.105	14.140	14.126	14.160	14.110	14.093	14.112
	11			14.317	14.329	14.353	14.394	14.321	14.356	14.285	14.377	14.330	14.309	14.328
	12			14.359	14.401	14.410	14.408	14.408	14.429	14.415	14.449	14.388	14.381	14.429
	13			14.374	14.416	14.410	14.408	14.408	14.443	14.429	14.464	14.388	14.381	14.429
	14			14.374	14.416	14.424	14.408	14.408	14.443	14.429	14.464	14.388	14.381	14.429
	15			14.374	14.416	14.410	14.408	14.408	14.443	14.429	14.464	14.388	14.381	14.429
	16			14.374	14.416	14.453	14.408	14.408	14.443	14.429	14.464	14.388	14.381	14.429
Wedge Probe	143.0	13.942	14.251	14.058	14.055	14.252	14.019	13.918	14.131	14.082	14.059	13.942	13.877	13.967
	243.5			14.075	14.069	14.123	14.077	14.062	14.443	14.082	14.132	14.028	13.949	14.040
	328.5	14.129	13.933	14.245	14.243	14.324	14.363	14.062	14.516	14.183	14.189	14.071	14.107	14.155
Kiel Probe	63.5	14.172	14.207	14.331	14.329	14.238	14.365	14.206	14.169	14.285	14.417	14.215	14.079	14.126
	219.0			14.374	14.416	14.367	14.408	14.379	14.443	14.530	14.464	14.388	14.381	14.429
	293.5	14.072	14.293	14.158	14.142	14.180	14.365	14.408	14.414	14.082	14.204	14.114	14.365	14.415
								Station 3A (Stator Exit)						
Wake Probe	358.8													
	1 (Tube No.)	14.345	14.351	14.317	14.387	14.353	14.380	14.379	14.415	14.429	14.435	14.330	14.323	14.357
	2	14.273	14.308	14.288	14.344	14.266	14.365	14.336	14.386	14.371	14.406	14.229	14.280	14.314
	3	14.287	14.308	14.259	14.272	14.238	14.308	14.293	14.363	14.357	14.363	14.258	14.295	14.357
	4	14.330	14.337	14.302	14.358	14.338	14.351	14.379	14.400	14.429	14.449	14.345	14.366	14.415
	5	14.359	14.366	14.345	14.369	14.338	14.365	14.379	14.400	14.443	14.465	14.345	14.366	14.435
	6	14.374	14.394	14.359	14.387	14.353	14.380	14.408	14.429	14.400	14.421	14.302	14.338	14.435
	7	14.374	14.365	14.144	14.358	14.195	14.409	14.365	14.400	13.822	13.944	13.683	14.007	14.336
	8	14.316	14.351	13.397	13.839	13.433	14.135	13.831	13.721	13.317	13.452	13.179	13.345	13.405
	9	14.186	14.236	13.411	13.565	13.289	13.495	13.442	13.346	13.014	13.061	12.863	12.943	13.002
	10	13.812	13.919	13.540	13.594	13.433	13.544	13.640	13.433	12.855	13.032	12.805	12.547	12.640
	11	13.381	13.501	13.828	14.416	13.606	13.775	13.946	13.664	12.985	14.449	12.920	12.368	12.525
	12	13.007	13.141	14.029	13.940	13.792	14.063	14.105	13.880	13.115	13.307	13.035	12.296	12.510
	13	12.762	12.939	14.158	14.069	13.950	14.250	14.221	14.025	13.346	13.509	13.349	12.310	12.525
	14	12.733	12.953	14.187	14.133	14.008	14.236	14.235	14.097	13.620	13.842	13.496	12.296	12.550
	15	12.992	13.155	14.302	14.199	11.537	14.351	14.322	14.030	14.154	14.218	13.913	12.382	12.698
	16	12.877	13.991	14.475	14.489	14.410	14.495	14.581	14.559	14.559	14.580	14.345	13.359	13.867
Wedge Probe	24.4	14.287	14.294	14.288	14.286	14.281	14.250	14.192	14.328	14.328	14.349	14.201	13.935	14.271
	65.8							14,221	13,773				14,223	14,271
	228.5	13.784	13.919	13.468	13.507	13.418	13.559	13.268	13.678	13.938	13.437	13.323	13.259	13.650
	328.8		14.294	14.331	14.387	14.281	14.322	14.336	14.400	14.342	15.202	14.345	14.338	14.329
Kiel Probe	13.8	13.553	13.529	14.202	14.315	14.170	14.178	14.365	13.723	14.386	14.392	14.302	13.359	13.622
	121.3	13.611	13.948	13.871	13.911	13.807	14.019	13.831	13.635	14.082	14.001	13.726	13.806	14.025
	280.5	14.316	14.337	14.288	14.372	14.338	13.674	14.394	14.385	14.371	14.319	14.086	14.323	14.329
	310.5	14.287	14.308	14.216	14.243	14.238	14.280	14.293	14.481	14.285	14.319	14.244	14.266	14.299

Table B-4. Wall Static Pressure, Weight Flow, Mach No., and Dynamic Pressure

Configuration	1	1A	2	5	7	9	15	18	4	6	8	10	14
Plenum Pressure	14.391	14.413	14.376	14.416	14.368	14.407	14.424	14.466	14.449	14.466	14.393	14.380	14.430
Tap Position, deg					Station 2 (Stator Inlet)								
193.5 ID	10.933	11.229	10.986	11.131	10.954	11.115	10.823	11.094	11.098	11.119	10.914	10.912	10.975
83.0 ID	10.859	11.131	10.837	11.035	10.565	10.707	10.262	10.620	10.503	10.371	10.320	10.357	10.356
3.0 ID	10.340	10.733	10.041	10.213	9.890	10.231	10.166	9.955	9.983	9.884	9.708	10.208	10.284
263.0 OD	11.381	11.634	11.440	11.644	11.452	11.586	11.659	11.558	11.531	11.562	11.424	11.455	11.487
133.0 OD	11.104	11.381	11.251	11.195	11.030	11.126	10.790	10.806	11.247	11.267	10.986	10.827	10.897
32.5 OD	11.471	11.789	11.463	11.361	11.249	11.479	11.560	11.433	11.482	11.495	8.805*	11.375	11.463
					Station 3A (Stator Exit)								
331.5 OD	12.150	12.323	12.066	12.051	11.982	12.187	12.061	12.035	12.088	12.114	8.808*	11.831	11.972
238.8 OD	12.018	12.319	12.028	12.177	11.990	12.182	12.070	11.923	12.103	12.213	8.807*	11.954	12.043
169.5 OD	12.006	12.275	12.056	12.080	12.963	12.183	12.000	11.894	12.163	12.175	8.807*	11.957	12.027
115.5 OD	12.054	12.369	12.154	12.140	12.036	12.246	11.992	12.003	12.263	12.223	12.004	12.004	12.151
61.5 OD	12.111	12.347	12.164	12.204	12.073	12.232	12.973	12.015	12.231	12.194	12.060	11.922	12.134
43.5 OD	12.257	12.505	12.401	12.348	12.266	12.448	12.126	12.231	12.391	12.343	12.173	12.109	12.252
7.5 OD	12.359	12.600	12.437	12.427	12.276	12.443	12.312	12.331	12.506	12.471	12.292	12.165	12.265
295.5 ID	12.014	12.247	11.989	11.963	11.833	12.068	12.013	11.955	12.034	12.074	11.807	11.781	11.932
193.9 ID	12.151	12.395	12.209	12.364	12.201	12.400	12.125	12.225	12.394	12.373	12.174	12.159	12.268
48.7 ID	12.230	12.462	12.281	12.342	12.246	12.397	12.054	12.195	12.349	12.290	12.146	12.085	12.239
$\dot{\omega}$, lb/sec	82.53	80.05	81.44	81.06	81.43	80.17	81.49	81.43	81.34	81.46	81.47	81.52	81.49
M_0	0.321	0.309	0.316	0.314	0.316	0.310	0.316	0.316	0.316	0.316	0.316	0.316	0.316
M_2	0.630	0.598	0.630	0.622	0.647	0.629	0.648	0.646	0.640	0.644	0.638	0.647	0.645
q_0, psia	0.984	0.920	0.959	0.947	0.959	0.925	0.959	0.959	0.959	0.959	0.959	0.959	0.959
q_2, psia	3.06	2.83	3.04	3.05	3.20	3.04	3.16	3.17	3.12	3.20	3.12	3.15	3.16

Pressure units are psia.

*Not used to obtain average values.

Table B-5. Stator Exit Air Angle, Midspan

Configuration	Circumferential Location, deg	Stator Exit Air Angle, Midspan, deg			
		24	65	228	328
Unslotted					
1		23.8		21.4	
1A		23.7		21.4	
Average		23.7			
Forward Slot					
2		23.5		21.9	
5		21.9		18.5	22.9
7		21.9		18.3	22.3
9		21.7		18.2	23.2
15		24.3*	21.9	20.0	21.9
18		21.2	22.4	21.2	22.6
Average		22.0			
Rear Slot					
4		21.6		21.3	22.2
6		21.7			22.6
8		23.9		18.9	22.8
10		21.4	22.8	19.3	24.4
14		18.6	21.9	19.0	19.9
Average		21.4			

*Not used to compute average.

APPENDIX C
BIBLIOGRAPHY

1. "The Theoretical and Experimental Analysis of the Tandem Axial Flow Blade Row," Railly, J. W., November 1964, Final Technical Report, Mechanical Engineering Dept., Univ. of Birmingham, Edgboston, Birmingham, England.

2. "Large-Scale Wind-Tunnel Tests and Evaluation of the Low-Speed Performance of a 35° Sweptback Wing Jet Transport Model Equipped with a Blowing Boundary-Layer-Control Flap and Leading-Edge Slat," Hickey, David H., and Kiyoshi Aoyagi. October 1960. (NASA Technical Note D-333.)

3. "Investigation of Double Slotted Flaps on a Swept-Wing Transport Model," Naeseth,Rodger L., and Edwin E. Davenport. October 1959. (NASA Technical Note D-103.)

4. "Boundary Layer Control in Short, Wide-Angle Diffusers by Use of Auxiliary Flow Injection with a Coanda Slot," Jones, B. A., December 1958, United Aircraft Research Department Report M-2000-41.

5. "Large-Scale Wind-Tunnel Tests of a Jet-Transport-Type Model with Leading- and Trailing-Edge High-Lift Devices," Hickey, David H., and Kiyoshi Aoyagi. September 1958. (NACA RM A58H12.)

6. "Surface Pressure Distributions on a Large-Scale 49° Sweptback Wing-Body-Tail Configuration with Blowing Applied Over the Flaps and Wing Leading Edge," McLemore, H. Clyde, and Marvin P. Fink. February 1958. (NACA RM L57K25.)

7. "Aerodynamic Characteristics of a Spoiler-Slot-Deflector Control on a 45° Sweptback Wing at Mach Numbers of 1.61 and 2.01," Lord, Douglas R., and Robert Moring. July 1957. (NACA RM L57E16a.)

8. "Exploratory Investigation of the Effect of Wing Slots and Leading-Edge Slats on the Longitudinal Stability Characteristics of a 45° Sweptback Wing-Fuselage Configuration," Critzos, Chris C. February 1957. (NACA RM L56L06.)

9. "Effect of Propeller Location and Flap Deflection on the Aerodynamic Characteristics of a Wing-Propeller Combination for Angles of Attack from 0° to 80°," Newsom, William A., Jr. January 1957. (NACA TN 3917.)

10. "Effects of Wing-Mounted External Stores on the Longitudinal and Lateral Handling Qualities of the Douglas D-558-II Research Airplane," Fischel, Jack, Robert W. Darville, and Donald Reisert. October 1957. (NACA RM H57H12.)

11. "Estimation of Incremental Pitching Moments Due to Trailing-Edge Flaps on Swept and Triangular Wings," James, Harry A., and Lynn W. Hunton. July 1957. (NACA TN 4040. Supersedes RM A55D07.)

12. "High-Pressure Blowing Over Flap and Wing Leading Edge of a Thin Large-Scale 49° Swept Wing-Body-Tail Configuration in Combination with a Drooped Nose and a Nose with a Radius Increase," Fink, Marvin P., and H. Clyde McLemore. May 1957. (NACA RM L57D23.)

13. "The Slotted-Blade Axial-Flow Blower," Sheets, H. E., November 1956, Trans. ASME.

14. "Blowing Over the Flaps and Wing Leading Edge of a Thin 49° Swept Wing-Body-Tail Configuration in Combination with Leading-Edge Devices," McLemore, H. Clyde, and Marvin P. Fink. July 1956. (NACA RM L56E16.)

15. "Effect of Several Wing Modifications on the Subsonic and Transonic Longitudinal Handling Qualities of the Douglas D-558-II Research Airplane," Fischel, Jack and Donald Reisert. June 1956. (NACA RM H56C30.)

16. "The Effects of Blowing Over Various Trailing-Edge Flaps on an NACA 0006 Airfoil Section, Comparisons with Various Types of Flaps on Other Airfoil Sections, and an Analysis of Flow and Power Relationships for Blowing Systems," Dods, Jules B., Jr., and Earl C. Watson. June 1956. (NACA RM A56C01.)

17. "Transonic Investigation of Aerodynamic Characteristics of a Swept-Wing Fighter-Airplane Model with Leading-Edge Droop in Combination with Outboard Chord-Extensions and Notches," Whitcomb, Charles F., and Harry T. Norton, Jr. March 1956. (NACA RM L55H30.)

18. "Aerodynamic Characteristics and Pressure Distributions of a 6-Percent-Thick 49° Sweptback Wing with Blowing Over Half-Span and Full-Span Flaps," Whittle, Edward F., Jr., and H. Clyde McLemore. September 1955. (NACA RM L55F02.)

19. "A Correlation of Two-Dimensional Data on Lift Coefficient Available with Blowing-, Suction-, Slotted-, and Plain-Flap High-Lift Devices," Riebe, John M. October 1955. (NACA RM L55D29a.)

20. "Effect of Several Wing Modifications on the Low-Speed Stalling Characteristics of the Douglas D-558-II Research Airplane," Fischel, Jack and Donald Reisert. July 1955. (NACA RM H55E31a).

21. "Estimation of Incremental Pitching Moments due to Trailing-Edge Flaps on Swept and Triangular Wings," James, Harry A. and Lynn W. Hunton. June 1955. (NACA RM A55D07).

22. "Full-Scale Wind Tunnel Tests of a 35° Sweptback Wing Airplane with High-Velocity Blowing Over the Trailing-Edge Flaps," Kelly, Mark W., and William H. Tolhurst, Jr. November 1955. (NACA RM A55I09).

23. "Effect on the Low-Speed Aerodynamic Characteristics of a 49° Sweptback Wing having an Aspect Ratio of 3.78 of Blowing Air over the Trailing-Edge Flap and Aileron," Whittle, Edward F. Jr., and Stanley Lipson. April 1954. (NACA RM L54C05).

24. "Effects of High-Lift Devices and Horizontal-Tail Location on the Low-Speed Characteristics of a Large-Scale 45° Swept-Wing Airplane Configuration," Maki, Ralph L. and Ursel R. Embry. August 1954. (NACA RM A54E10).

25. "Low-Speed Chordwise Pressure Distributions Near the Midspan Station of the Slotted Flap and Aileron of a 1/4-Scale Model of the Bell X-1 Airplane with a 4-Percent-Thick, Aspect-Ratio-4, Unswept Wing," Moseley, William C. Jr. and Robert T. Taylor. March 1954. (NACA RM L53L18).

26. "Static Longitudinal Stability Characteristics of a Composite-Plan-Form Wing Model Including some Comparisons with a 45° Sweptback Wing at Transonic Speeds," Wolhart, Walter D. August 1954. (NACA RM L54F24).

27. "Wind-Tunnel Investigation at High Subsonic Speeds of the Stability Characteristics of a Complete Model having Sweptback-, M-, W-, and Cranked-Wing Plan Forms and Several Horizontal-Tail Locations," Goodson, Kenneth W. and Robert E. Becht. May 1954. (NACA RM L54C29).

28. "Wind-Tunnel Investigation at Low Speed of the Effects of Chordwise Wing Fences and Horizontal-Tail Position on the Static Longitudinal Stability Characteristics of an Airplane Model with a 35° Sweptback Wing," Queijo, M. J., Byron M. Jaquet, and Walter D. Wolhart. 1954. (NACA Rept. 1203. Supersedes RM L50K07; RM L51H17).

29. "Investigation of the Effects of Wing and Tail Modifications on the Low-Speed Stability Characteristics of a Model having a Thin 40° Swept Wing of Aspect Ratio 3.5," Weil, Joseph, William C. Sleeman, Jr., and Andrew L. Byrnes, Jr. April 1953. (NACA RM L53C09).

30. "Lift and Pitching Moment at Low Speeds of the NACA 64A010 Airfoil Section Equipped with Various Combinations of a Leading-Edge Slat, Leading-Edge Flap, Split Flap, and Double-Slotted Flap," Kelly, John A. and Nora-Lee F. Hayter. September 1953. (NACA TN 3007).

31. "The Use of Area Suction for the Purpose of Improving Trailing-Edge Flap Effectiveness on a 35° Sweptback Wing," Cook, Woodrow L., Curt A. Holzhauser, and Mark W. Kelly. July 1953. (NACA RM A53E06).

32. "Effect of High-Lift Devices on the Static-Lateral-Stability Derivatives of a 45° Sweptback Wing of Aspect Ratio 4.0 and Taper Ratio 0.6 in Combination with a Body," Lichtenstein, Jacob H. and James L. Williams. November 1952. (NACA TN 2819).

33. "Effects of Several High-Lift and Stall-Control Devices on the Aerodynamic Characteristics of a Semispan 49° Sweptback Wing," Barnett, U. Reed, Jr., and Stanley Lipson. September 1952. (NACA RM L52D17a).

34. "Full-Scale Wind-Tunnel Investigation of the Effects of Wing Modifications and Horizontal-Tail Location on the Low-Speed Static Longitudinal Characteristics of a 35° Swept-Wing Airplane," Maki, Ralph L. April 1952. (NACA RM A52B05).

57. "Lateral-Control Investigation on a 37° Sweptback Wing of Aspect Ratio 6 at a Reynolds Number of 6,800,000," Graham, Robert R. and William Koven. January 27, 1949. (NACA RM L8K12).

58. "Summary of Section Data on Trailing-Edge High-Lift Devices," Cahill, Jones F. 1949. (NACA Rept. 938).

59. "Two-Dimensional Wind-Tunnel Investigation of a 6-Percent-Thick Symmetrical Circular-Arc Airfoil Section with Leading-Edge and Trailing-Edge High-Lift Devices Deflected in Combination," Nuber, Robert J. and Gail A. Cheesman. September 6, 1949. (NACA RM L9G20).

60. "The Effect of Boundary-Layer Control by Suction and of Several High-Lift Devices on the Aerodynamic Characteristics in Yaw of a 47.5° Sweptback Wing-Fuselage Combination," Pasamanick, Jerome. October 28, 1948. (NACA RM L8E21).

61. "The Effects of High-Lift Devices on the Low-Speed Stability Characteristics of a Tapered 37.5° Sweptback Wing of Aspect Ratio 3 in Straight and Rolling Flow," Queijo, M. J. and Jacob H. Lichtenstein. November 9, 1948. (NACA RM L8I03).

62. "High-Speed Stability and Control Characteristics of a Fighter Airplane Model with a Swept-Back Wing and Tail," Morrill, Charles P. Jr., and Lee E. Boddy. April 14, 1948. (NACA RM A7K28).

63. "Longitudinal Stability Characteristics of a 42° Sweptback Wing and Tail Combination at a Reynolds Number of 6.8 x 10^6. Spooner, Stanley H. and Albert P. Martina. July 22, 1948. (NACA RM L8E12).

64. "Wind-Tunnel Investigation of Boundary-Layer Control by Suction on NACA 65-424 Airfoil with Double Slotted Flap," Racisz, Stanley F. and John H. Quinn, Jr. June 1948. (NACA TN 1631).

65. "Wind-Tunnel Investigation of High-Lift and Stall-Control Devices on a 37° Sweptback Wing of Aspect Ratio 6 at High Reynolds Numbers," Koven, William and Robert R. Graham. September 2, 1948. (NACA RM L8D29).

66. "Aerodynamic Data for a Wing Section of the Republic XF-12 Airplane Equipped with a Double Slotted Flap," Cahill, Jones F. January 1946. (NACA RM L6A08a).

67. "Drag Tests of an NACA $65_{(215)}$-114, α = 1.0 Practical-Construction Airfoil Section Equipped with a 0.295-Airfoil-Chord Slotted Flap," Quinn, John H., Jr. April 1947. (NACA TN 1236).

68. "Investigation of High-Lift and Stall-Control Devices on an NACA 64-Series 42° Sweptback Wing with and without Fuselage," Graham, Robert R. and D. William Conner. October 14, 1947. (NACA RM L7G09).

35. "An Investigation of a 0.16-Scale Model of the Douglas X-3 Airplane to Determine Means of Improving the Low-Speed Longitudinal Stability and Control Characteristics," McKee, John W. and John M. Riebe. November 1952. (NACA RM L52H01).

36. "Low-Speed Aerodynamic Characteristics of a Large-Scale 45° Swept-Back Wing with Partial-Span Slats, Double-Slotted Flaps, and Ailerons," James, Harry A. April 1952. (NACA RM A52B19).

37. "Low-Speed Aerodynamic Characteristics of a Large-Scale 60° Swept-Back Wing with High Lift Devices," Kelly, Mark W. March 1952. (NACA RM A52A14a).

38. "A Summary and Analysis of the Low-Speed Longitudinal Characteristics of Swept Wings at High Reynolds Number," Furlong, G. Chester and James G. McHugh. August 1952. (NACA RM L52D16).

39. "Wind-Tunnel Tests on the 30 Percent Symmetrical Griffith Aerofoil with Ejection of Air at the Slots," Gregory, N., W. S. Walker, and W. G. Raymer. Gt. Brit., Aeronautical Research Council, Reports and Memoranda No. 2475, 1952 (November 18, 1946). British Information Services, New York.

40. "Effect of Vertical-Tail Area and Length on the Yawing Stability Characteristics of a Model Having a 45° Sweptback Wing," Letko, William. May 1951. (NACA TN 2358).

41. "Experimental Investigation of the Effect of Vertical-Tail Size and Length and of Fuselage Shape and Length on the Static Lateral Stability Characteristics of a Model with 45° Sweptback Wing and Tail Surfaces," Queijo, M. J. and Walter D. Wolhart. 1951. (NACA Rept. 1049, Formerly TN 2168).

42. "Investigation at Low Speed of 45° and 60° Sweptback, Tapered, Low-Drag Wings, Equipped with Various Types of Full-Span, Trailing-Edge Flaps," Harper, John J.,Georgia Institute of Technology. October 1951. (NACA TN 2468).

43. "Pressure Distribution at Low Speed on a 1/4-Scale Bell X-5 Airplane Model," Kemp, William B. Jr. and Albert G. Few, Jr. December 1951. (NACA RM L51I25).

44. "A Study of the Use of Experimental Stability Derivatives in the Calculation of the Lateral Disturbed Motions of a Swept-Wing Airplane and Comparison with Flight Results," Bird, John D. and Byron M. Jaquet. 1951. (NACA Rept. 1031. Formerly TN 2013).

45. "Wind-Tunnel Investigation of the Effects of Horizontal-Tail Position on the Low-Speed Longitudinal Stability Characteristics of an Airplane Model with a 35° Sweptback Wing Equipped with Chordwise Fences," Queijo, M. J. and Walter D. Wolhart. November 1951. (NACA RM L51H17).

46. "Experimental Investigation of the Effect of Vertical-Tail Size and Length and of Fuselage Shape and Length on the Static Lateral Stability Characteristics of a Model with 45° Sweptback Wing and Tail Surfaces," Queijo, M. J. and Walter D. Wolhart. August 1950. (NACA TN 2168).

47. "Investigation of Boundary-Layer Control to Improve the Lift and Drag Characteristics of the NACA 65_2-415 Airfoil Section with Double Slotted and Plain Flaps," Horton, Elmer A., Stanley F. Racisz, and Nicholas J. Paradiso. August 1950. (NACA TN 2149).

48. "Low-Speed Lateral Stability and Aileron-Effectiveness Characteristics at a Reynolds Number of 3.5×10^6 of a Wing with Leading-Edge Sweepback Decreasing from 45° at the Root to 20° at the Tip," Lange, Roy H. and Huel C. McLemore. July 6, 1950. (NACA RM L50D14).

49. "Maximum Lift and Longitudinal Stability Characteristics at Reynolds Numbers up to 7.8×10^6 of a 35° Sweptforward Wing Equipped with High-Lift and Stall-Control Devices, Fuselage, and Horizontal Tail," Martina, Albert P. and Owen J. Deters. February 9, 1950. (NACA RM L9H18a).

50. "Maximum-Lift Characteristics of a Wing with the Leading-Edge Sweepback Decreasing from 45° at the Root to 20° at the Tip at Reynolds Numbers from 2.4×10^6 to 6.0×10^6," Lange, Roy H. July 6, 1950. (NACA RM L50A04a).

51. "Positioning Investigation of Single Slotted Flaps on a 47.7° Sweptback Wing at Reynolds Numbers of 4.0×10^6 and 6.0×10^6," Spooner, Stanley H. and Ernst F. Mollenberg. October 9, 1950. (NACA RM L50H29).

52. "Stability and Control Characteristics of a 1/4-Scale Bell X-5 Airplane Model in the Landing Configuration," Becht, Robert E. December 18, 1950. (NACA RM L50J27).

53. "Stability and Control Characteristics at Low Speed of a 1/4-Scale Bell X-5 Airplane Model. Lateral and Directional Stability and Control," Kemp, William B. Jr. and Robert E. Becht. June 20, 1950. (NACA RM L50C17a).

54. "Stability and Control Characteristics at Low Speed of a 1/4-Scale Bell X-5 Airplane Model. Longitudinal Stability and Control," Kemp, William B. Jr., Robert E. Becht and Albert G. Few, Jr. March 14, 1950. (NACA RM L9K08).

55. "A Study of the Use of Experimental Stability Derivatives in the Calculation of the Lateral Disturbed Motions of a Swept-Wing Airplane and Comparison with Flight Results," Bird, John D. and Byron M. Jaquet. January 1950. (NACA TN 2013).

56. "An Investigation of the Spin and Recovery Characteristics of a 1/25-Scale Model of the Douglas D-558-II Airplane," Scher, Stanley H. and Lawrence J. Gale. January 18, 1949. (NACA RM L8K19a).

69. "Tests of the NACA 64_1A212 Airfoil Section with a Slat, a Double Slotted Flap, and Boundary-Layer Control by Suction," Quinn, John H.,Jr. May 1947. (NACA TN 1293).

70. "Two-Dimensional Wind-Tunnel Investigation of Four Types of High-Lift Flap on an NACA 65-210 Airfoil Section," Cahill, Jones F. February 1947. (NACA TN 1191).

71. "Wind-Tunnel Tests at Low Speed of Swept and Yawed Wings having Various Plan Forms," Purser, Paul E. and M. Leroy Spearman. May 1947 (NACA RM L7D23).

72. "Wind-Tunnel Investigation of the NACA 654-421 Airfoil Section with a Double Slotted Flap and Boundary-Layer Control by Suction," Quinn, John H. Jr. July 1947. (NACA TN 1395).

73. "Two-Dimensional Wind-Tunnel Investigation of Two NACA Low-Drag Airfoil Sections Equipped with Slotted Flaps and a Plain NACA Low-Drag Airfoil Section for XF6U-1 Airplane," Loftin, Lawrence K., Jr. and Fred J. Rice, Jr. January 1946. (NACA MR L5L11).

74. "Lift Tests of a 0.1536c Thick Douglas Airfoil Section of NACA 7-Series Type Equipped with a Lateral-Control Device for Use with a Full-Span Double-Slotted Flap on the C-74 Airplane," Nuber, Robert J. and Fred J. Rice, Jr. March 1945. (NACA MR L5C24a).

75. "Effect of Compressibility on Pressure Distribution over an Airfoil with a Slotted Frise Aileron," Luoma, Arvo A. July 1944. (NACA Advance Confidential Report No. L4G12).

76. "Tests of a Griffith Aerofoil in the 13 ft x 9 ft Wind Tunnel,"
I - Wind Tunnel Technique and Interim Note. E. J. Richards.
II - Effect of Concavity on Drag. E. J. Richards, W. S. Walker, and J. R. Greening.
III - The Effects of Wide Slots and of Premature Transition to Turbulence - E. J. Richards and W. S. Walker.
IV - Lift, Drag, Pitching Moments and Velocity Distributions - E. J. Richards and W. S. Walker.
Great Britain, Aeronautical Research Council, Reports and Memoranda, No. 2148, March 1944.

77. "Effect of Wing Leading-Edge Slots on the Spin and Recovery Characteristics of Airplanes," Neihouse, Anshal I. and Marvin Pitkin. April 1943. (NACA Advance Restricted Report No. 3D29).

78. "Test of NACA 66,2-116, a = 0.6 Airfoil Section Fitted with Pressure Balance and Slotted Flaps for the Wing of the XP-63 Airplane," Underwood, William J. and Frank T. Abbott, Jr. May 1942. (NACA Memorandum Report). (Wartime Report No. L-701).

79. "Wind Tunnel Investigation of an NACA 23012 Airfoil with a Handley Page Slot and Two Flap Arrangements," Schuldenfrei, Marvin J. February 1942 (NACA Advanced Restricted Report). (Wartime Report No. L-261)

80. "Wind Tunnel Investigation of a Tapered Wing with a Plug-Type Spoiler-Slot Aileron and Full-Span Slotted Flaps," Lowry, John G. and Robert B. Liddell. July 1942. (NACA Advance Restricted Report). (Wartime Report No. L-250).

81. "Lift and Drag Characteristics of a Low-Drag Airfoil with Slotted Flap Submitted by Curtiss-Wright Corporation," Abbott, I. H. December 1941. (NACA Memorandum Report). (Wartime Report No. L-703).

82. "Wind Tunnel Investigation of a Plain and a Slot-Lip Aileron on a Wing with a Full-Span Flap Consisting of an Inboard Fowler and an Outboard Slotted Flap," Rogallo, F. M. and Marvin Schuldenfrei. June 1941 (NACA Advance Restricted Report). (Wartime Report No. L-421).

83. "Wind-Tunnel Investigation of a Spoiler-Slot Aileron on an NACA 23012 Airfoil with a Full-Span Fowler Flap," Rogallo, F. M. and Bartholomew S. Spano. December 1941. (NACA Advance Restricted Report). (Wartime Report No. L-376).

84. "Free Streamline Suction Slots," Watson, E. J. Great Britain Aeronautical Research Council, Reports and Memoranda No. 2177, February 1946.

85. "Tests on an Aerofoil with 20 Percent Slotted Flap and an Auxiliary Flap in the Compressed Air Tunnel," Jones, R. and A. H. Bell. Great Britain Aeronautical Research Council, Reports and Memoranda No. 2101. June 1939.

86. NPL Aerofoil Catalogue and Bibliography, by Pankhurst, R. C. 1952. CP No. 81, July 14, 1951. Great Britain Aeronautical Research Committee.

87. NPL Aerofoil Catalogue and Bibliography, by Pankhurst, R. C. R&M No. 3311, March 1962, issued 1963. Great Britain Aeronautical Research Committee.

APPENDIX D
ILLUSTRATIONS

Figures in the following pages are presented as cited in this report.

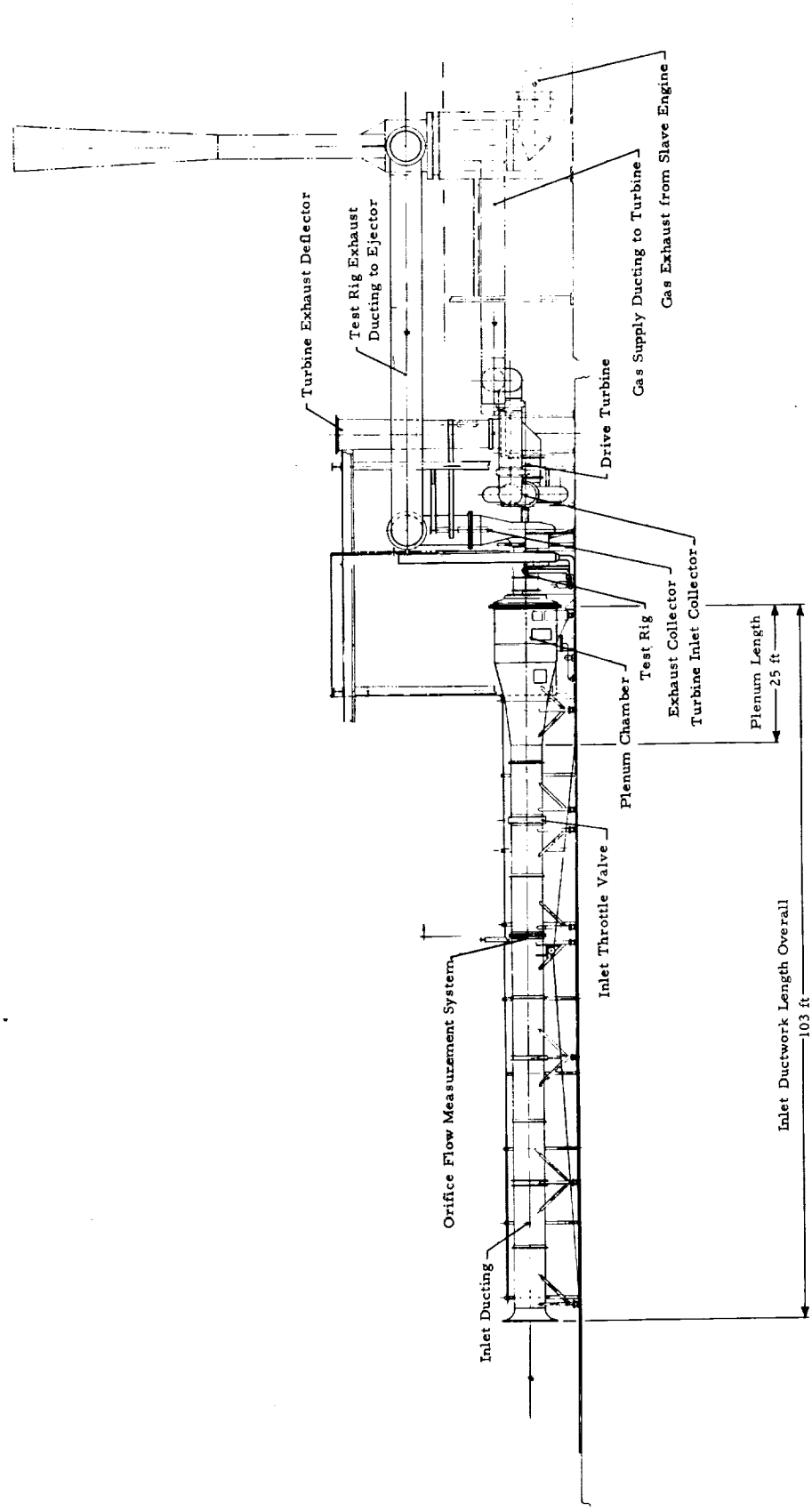

FD 10891A

Figure III-1. Schematic of the Compressor Research Facility

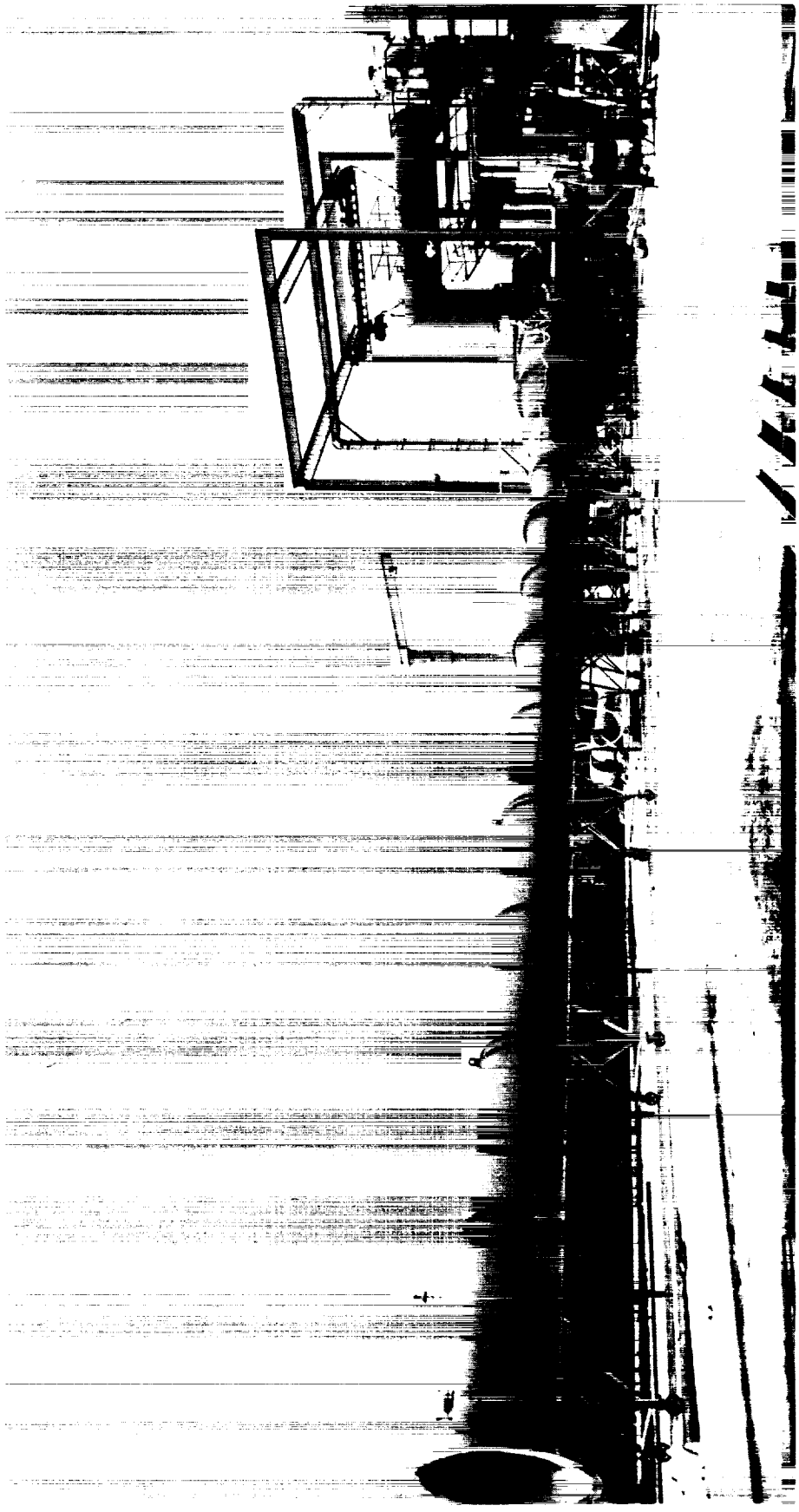

FE 51208

Figure III-2. Compressor Research Facility

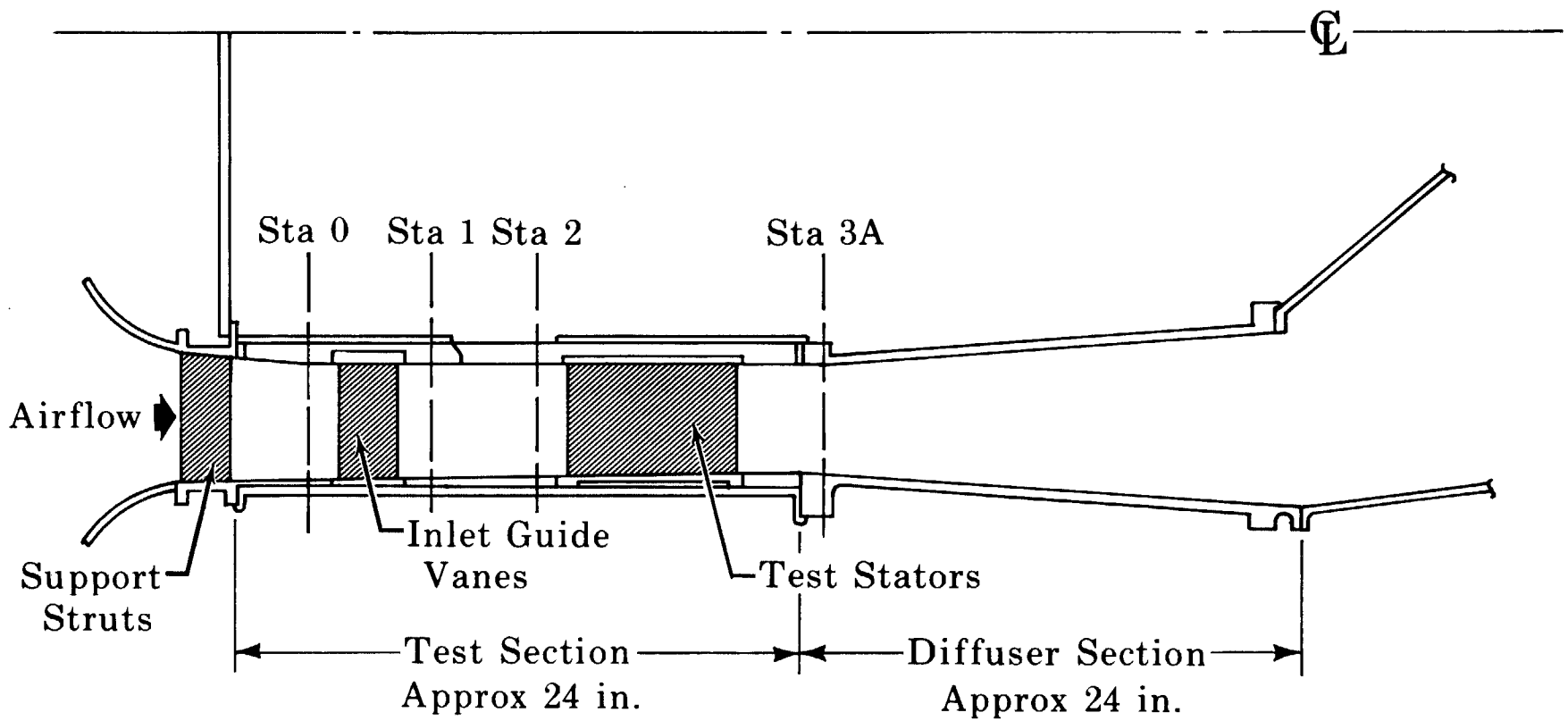

Measuring Station Diameters - in.

Station	ID	OD
0	32.38	41.12
1	32.85	40.57
2	32.85	40.23
3A	32.85	39.99

Figure III-3.. Schematic of Annular Cascade Rig

FD 14997B

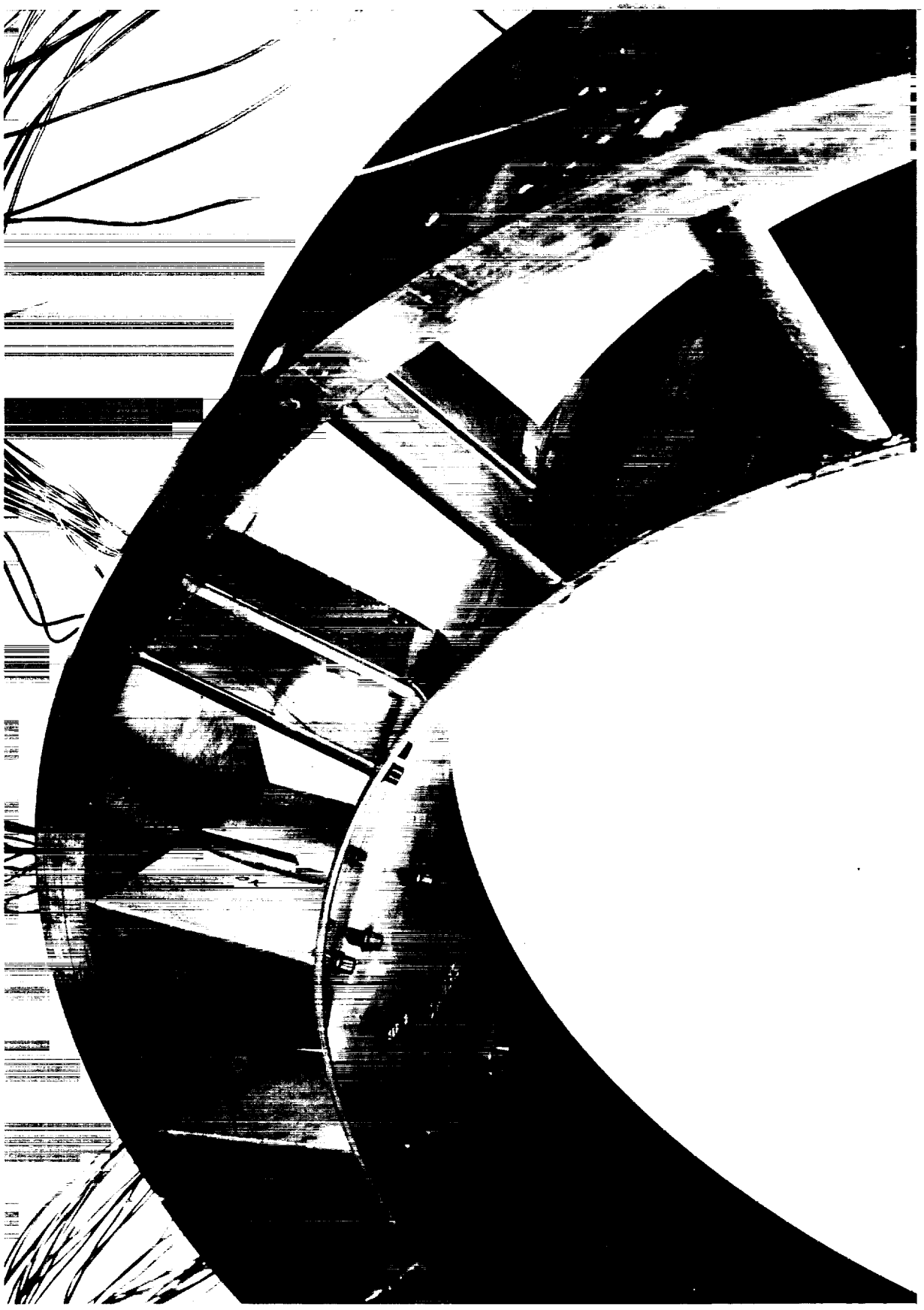

FE 53351

Figure III-4. Stator Vane Assembly

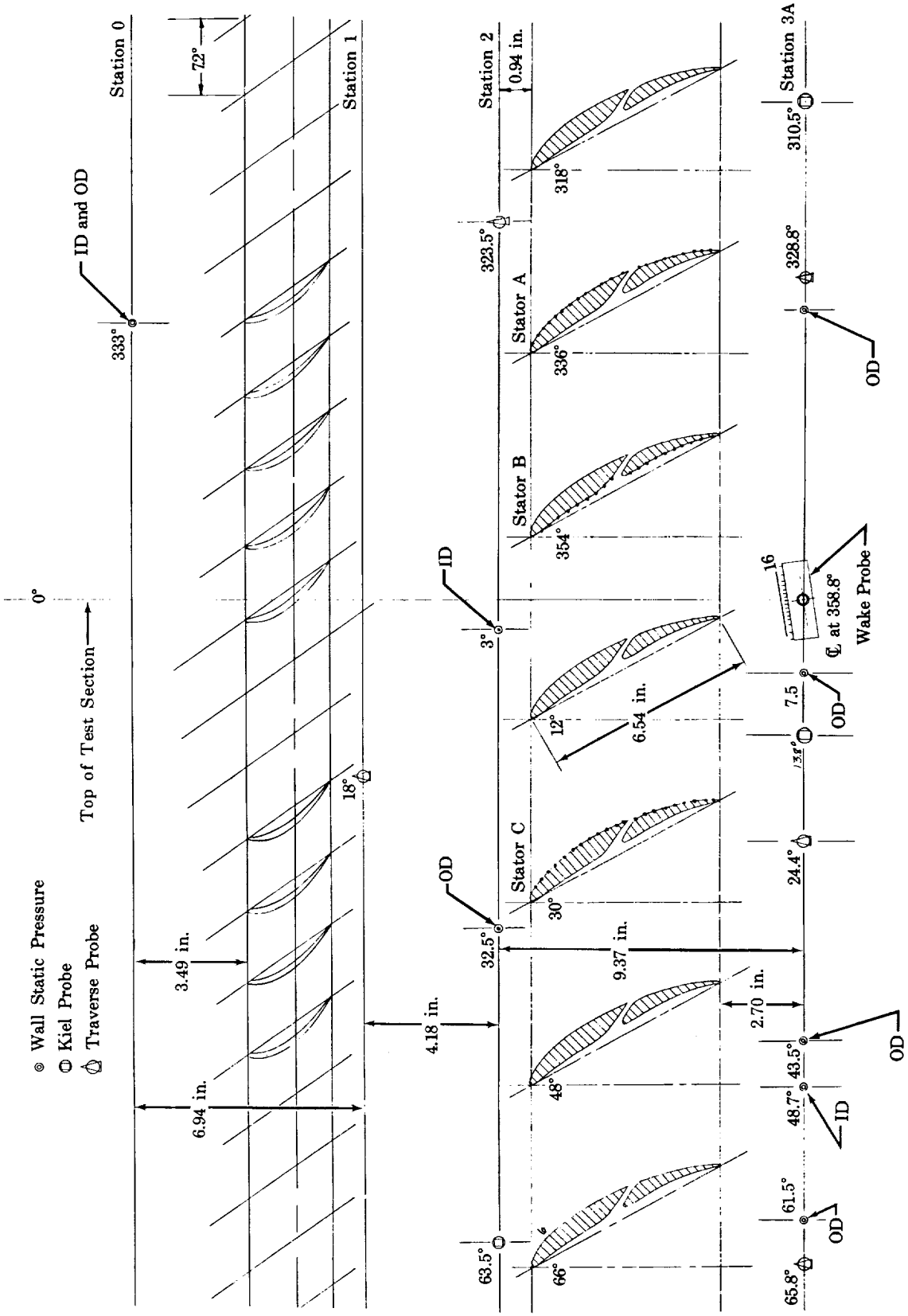

FD 14973B

Figure III-5. Test Section Instrumentation Layout

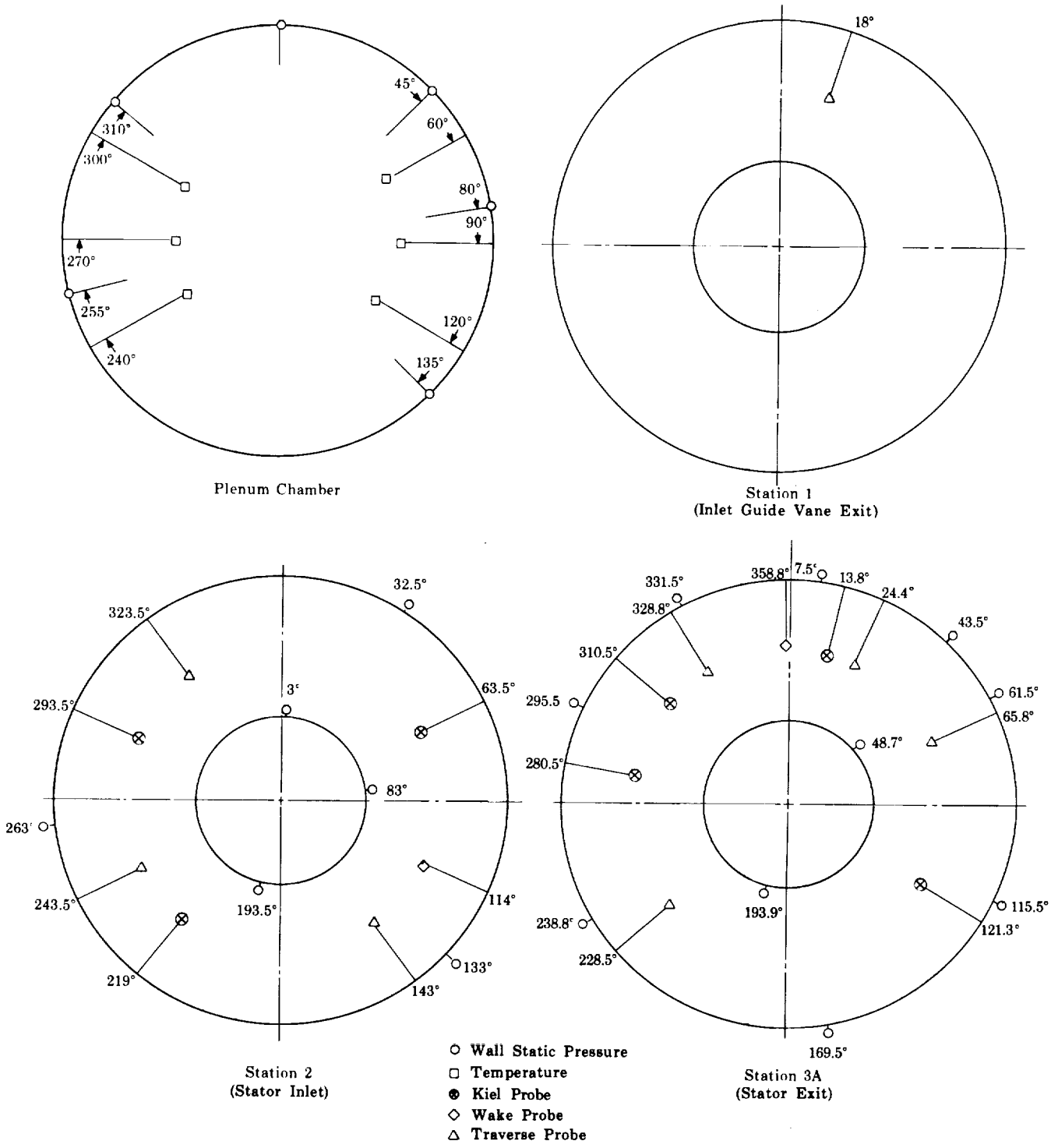

Figure III-6. Instrumentation, Plenum Chamber and Stations 1, 2, and 3A (View Looking Downstream) FD 14975A

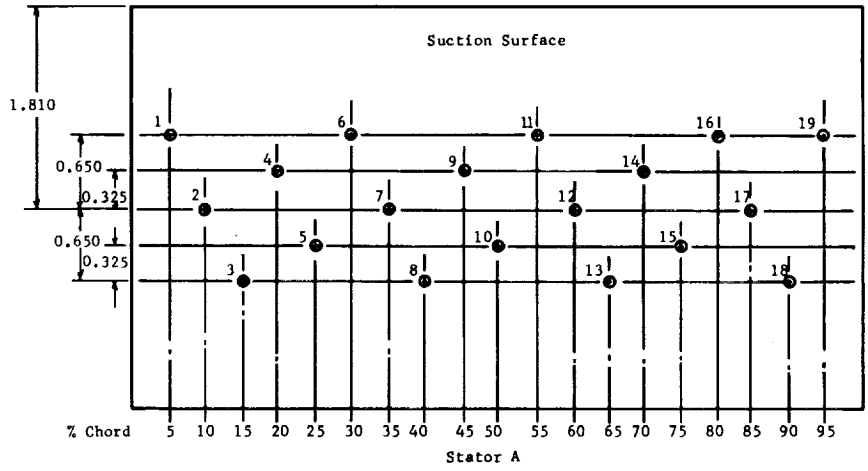

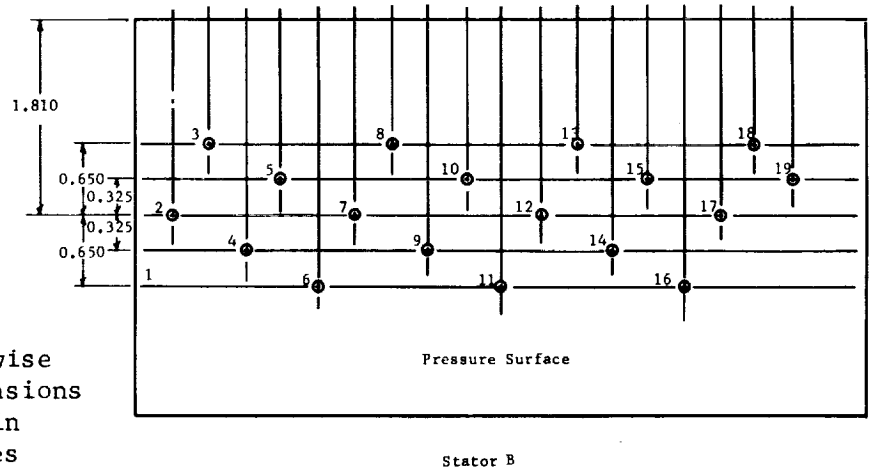

Note: Spanwise dimensions are in inches

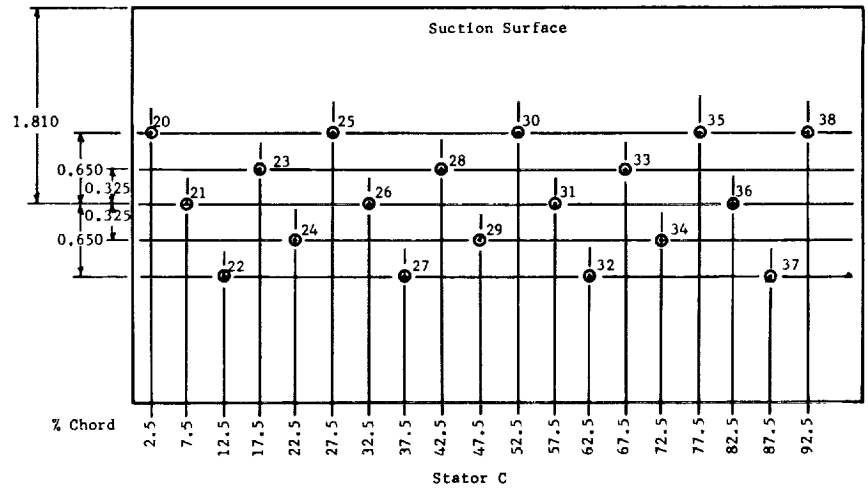

Figure III-7. Stator Surface Pressure Tap Locations FD 14998

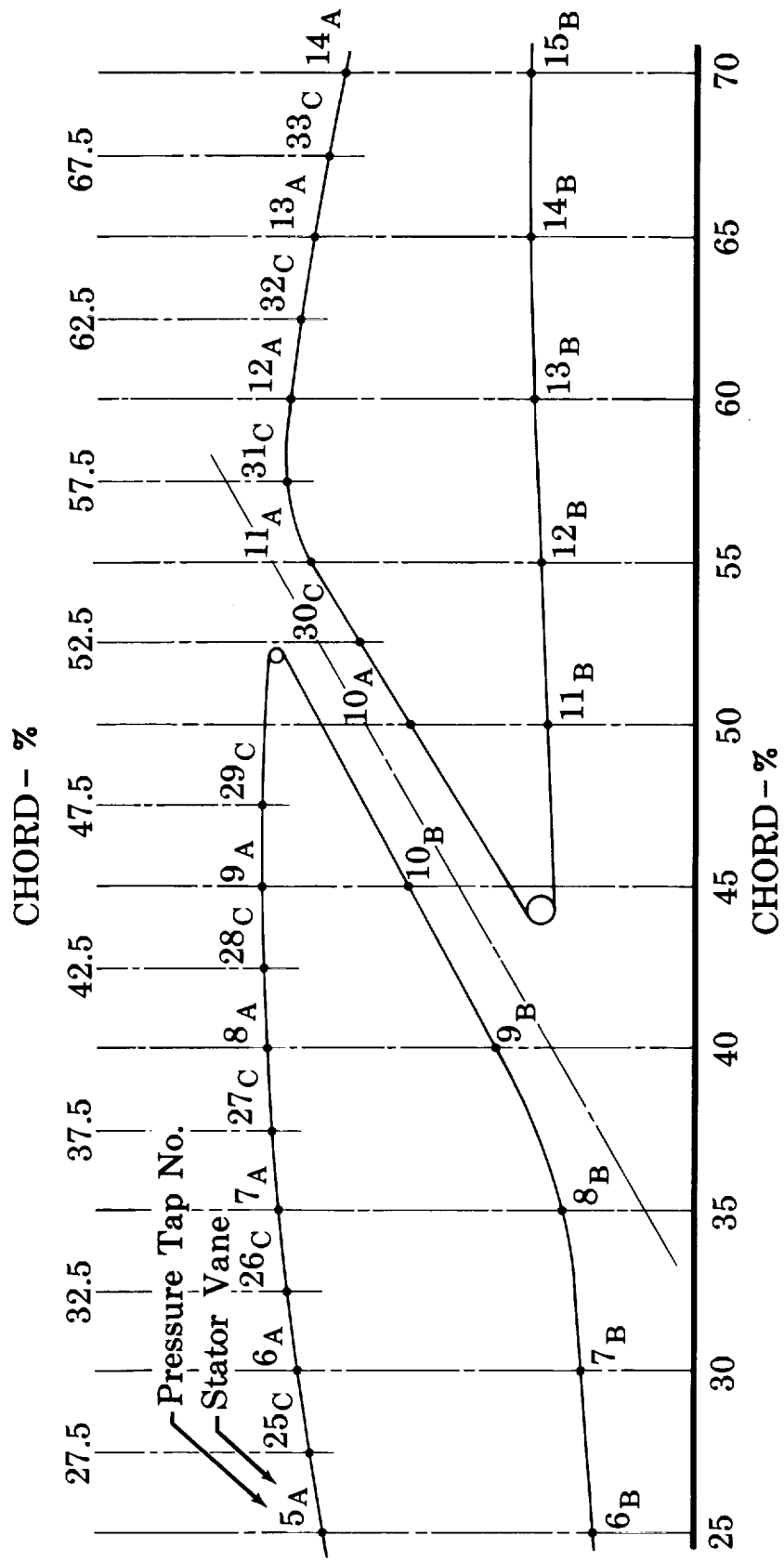

FD 14976A

Figure III-8. Static Pressure Tap Locations Near Forward Slot

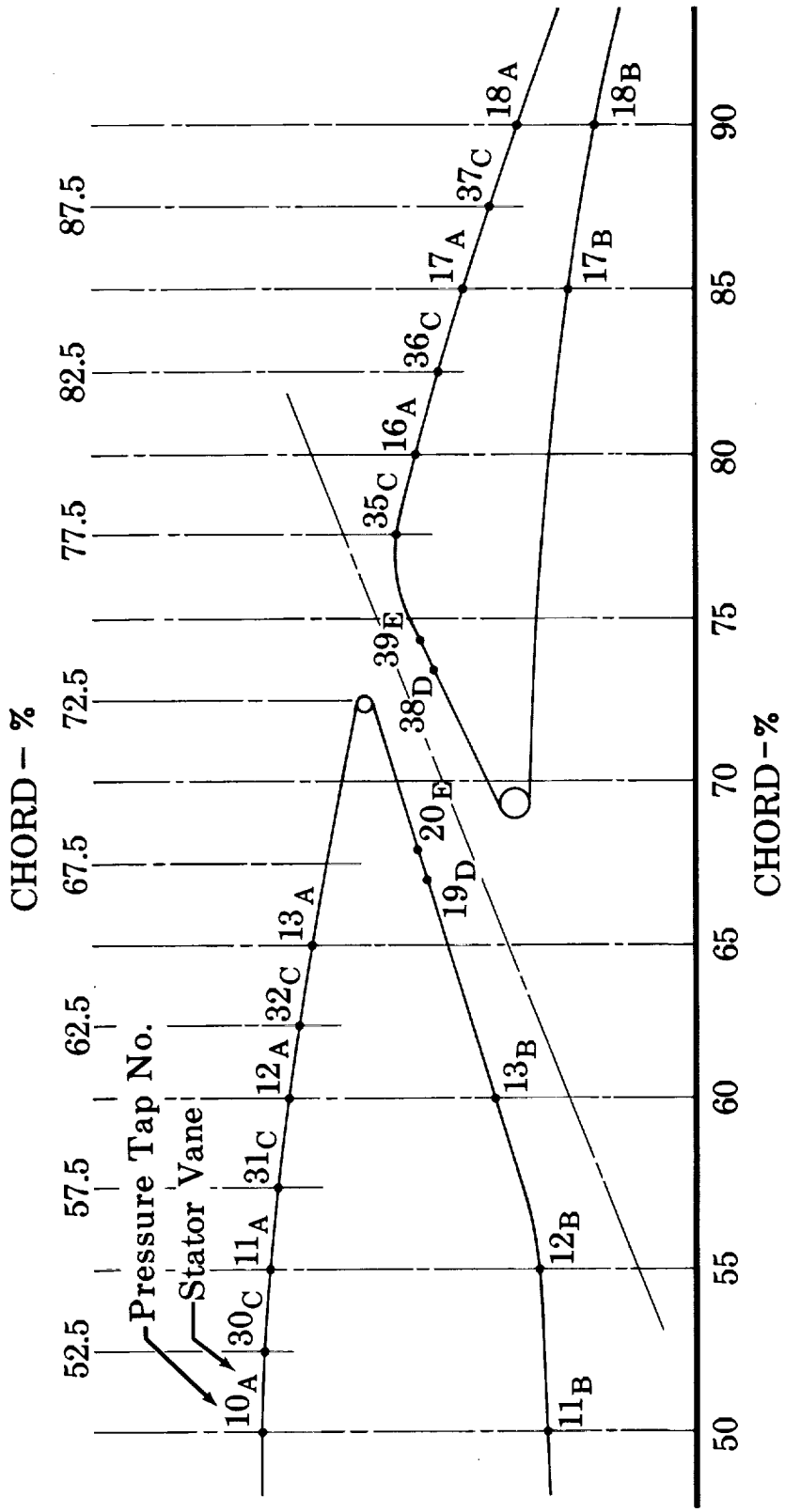

FD 14974A

Figure III-9. Static Pressure Tap Locations Near Rear Slot

Hypo Tubing Sealed into
Grooves with Epoxy

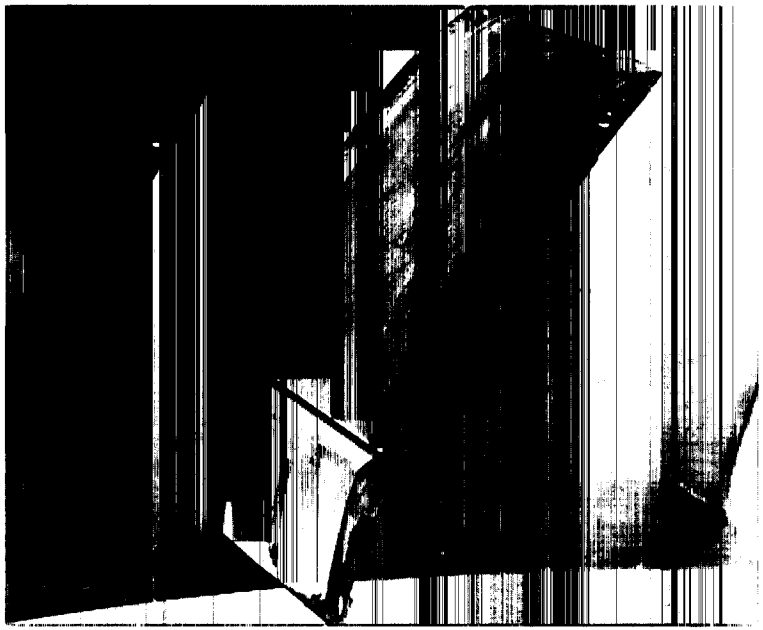

Pressure Taps Drilled into
Sealed Grooves from Opposite Surface

Figure III-10. Static Pressure Tap Installation

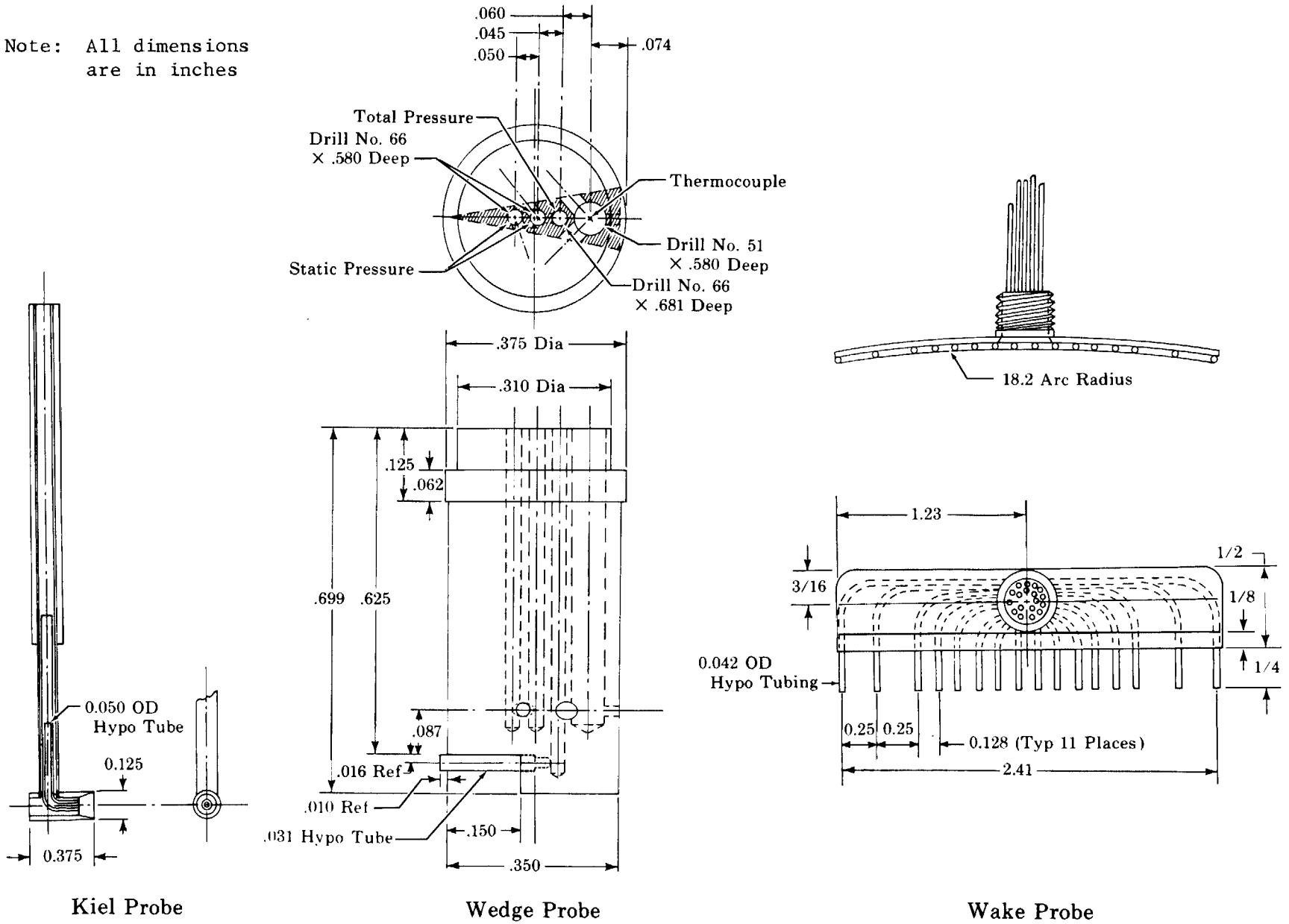

Figure III-11. Total Pressure Probes

FD 14977A

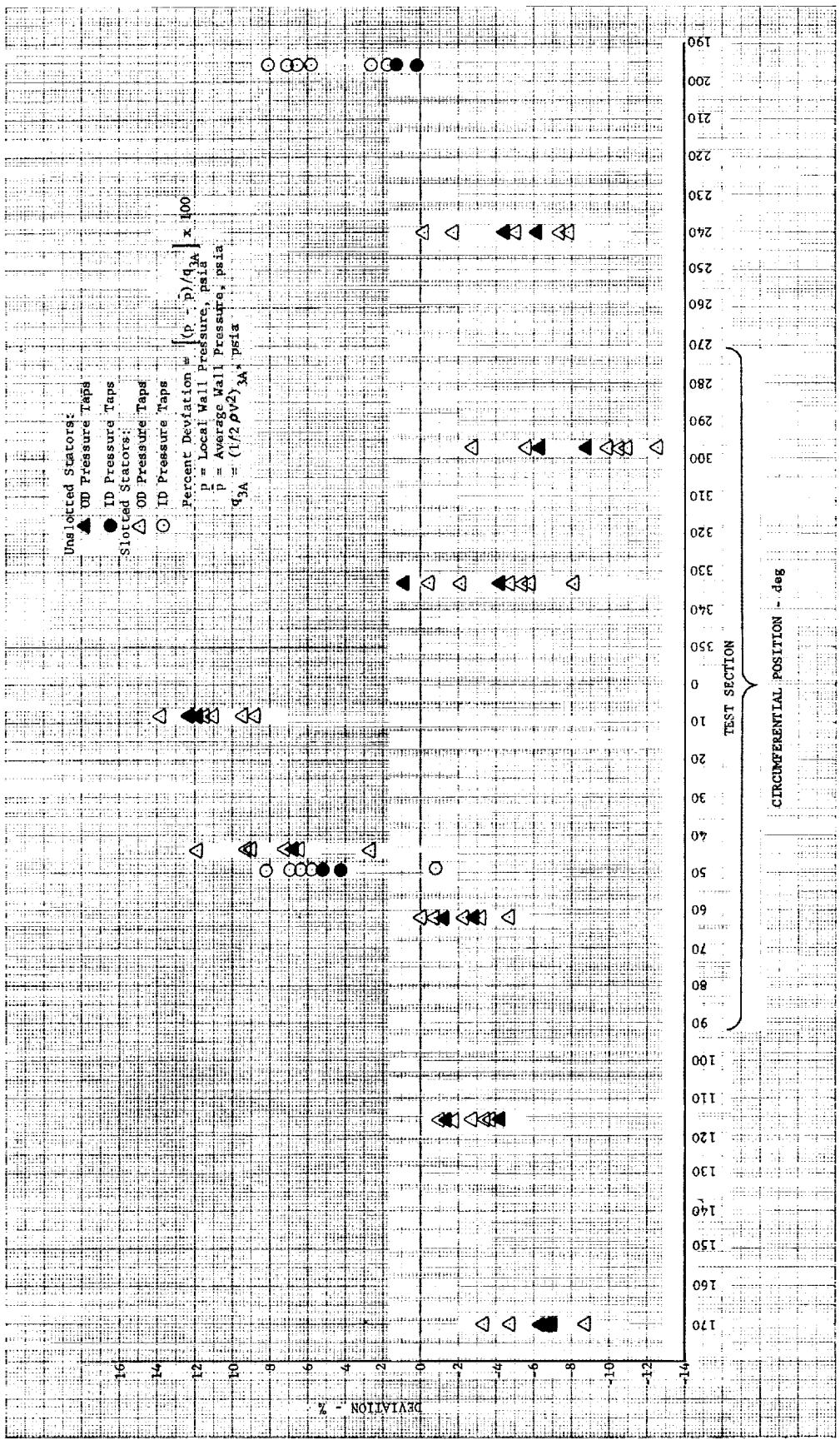

Figure IV-1. Circumferential Static Pressure Deviation at Station 3A (Forward Slot Configurations) DF 45542

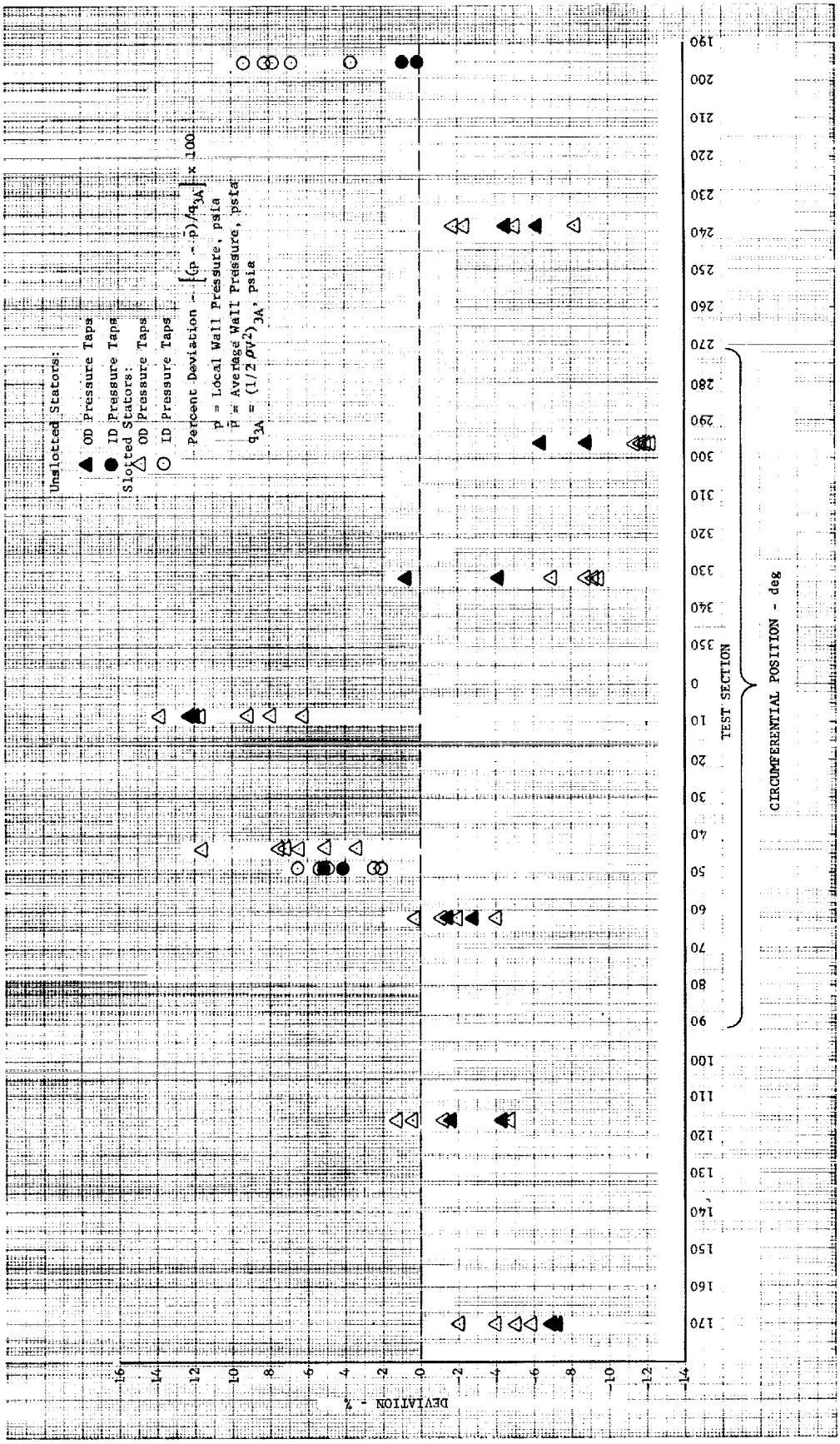

Figure IV-2. Circumferential Static Pressure Deviation at Station 3A (Rear Slot Configurations) DF 45539

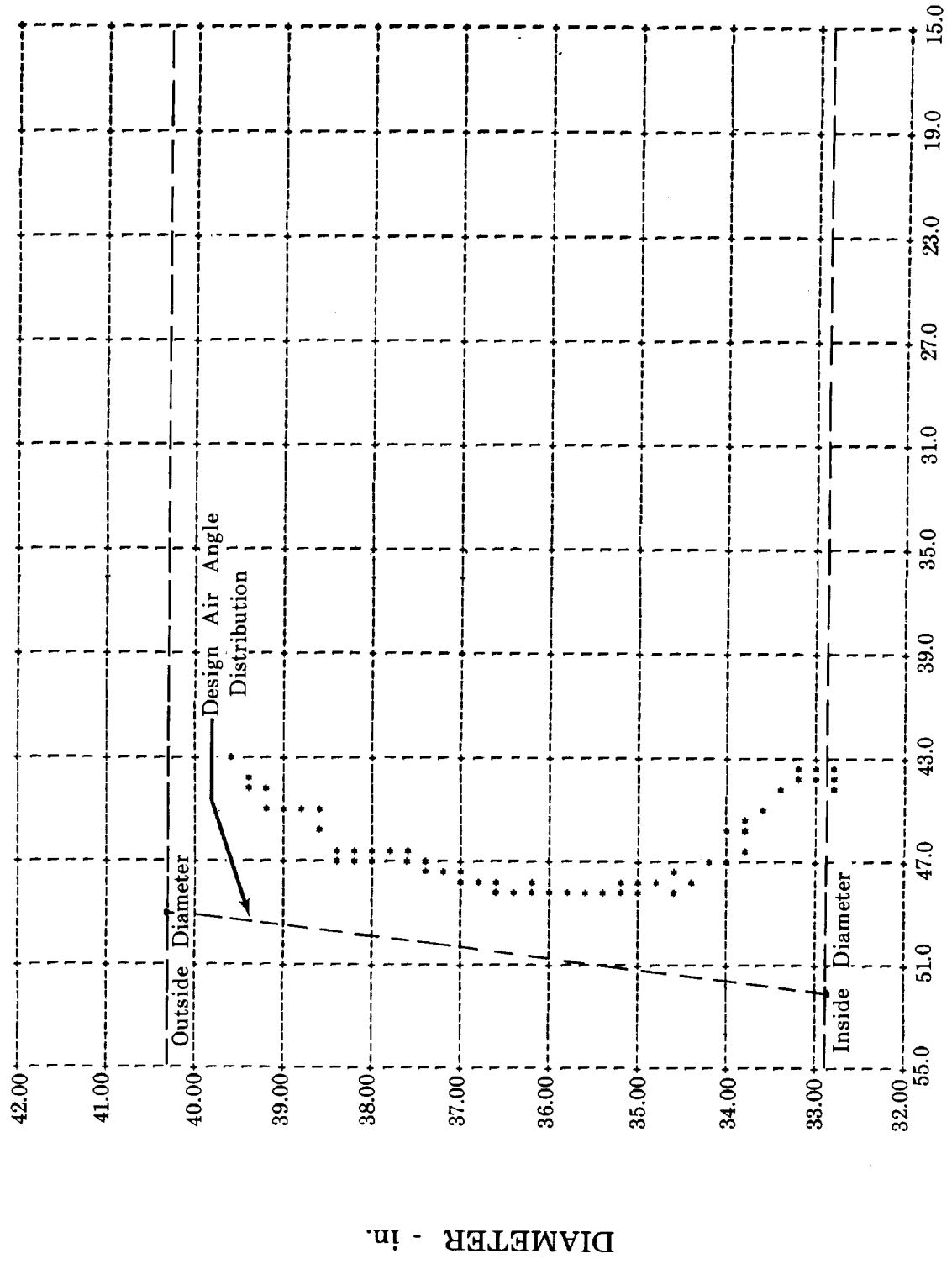

Figure V-1. IBM Plot of Stator Inlet Air Angle Profile, Configuration 1, Station 2

FD 17444A

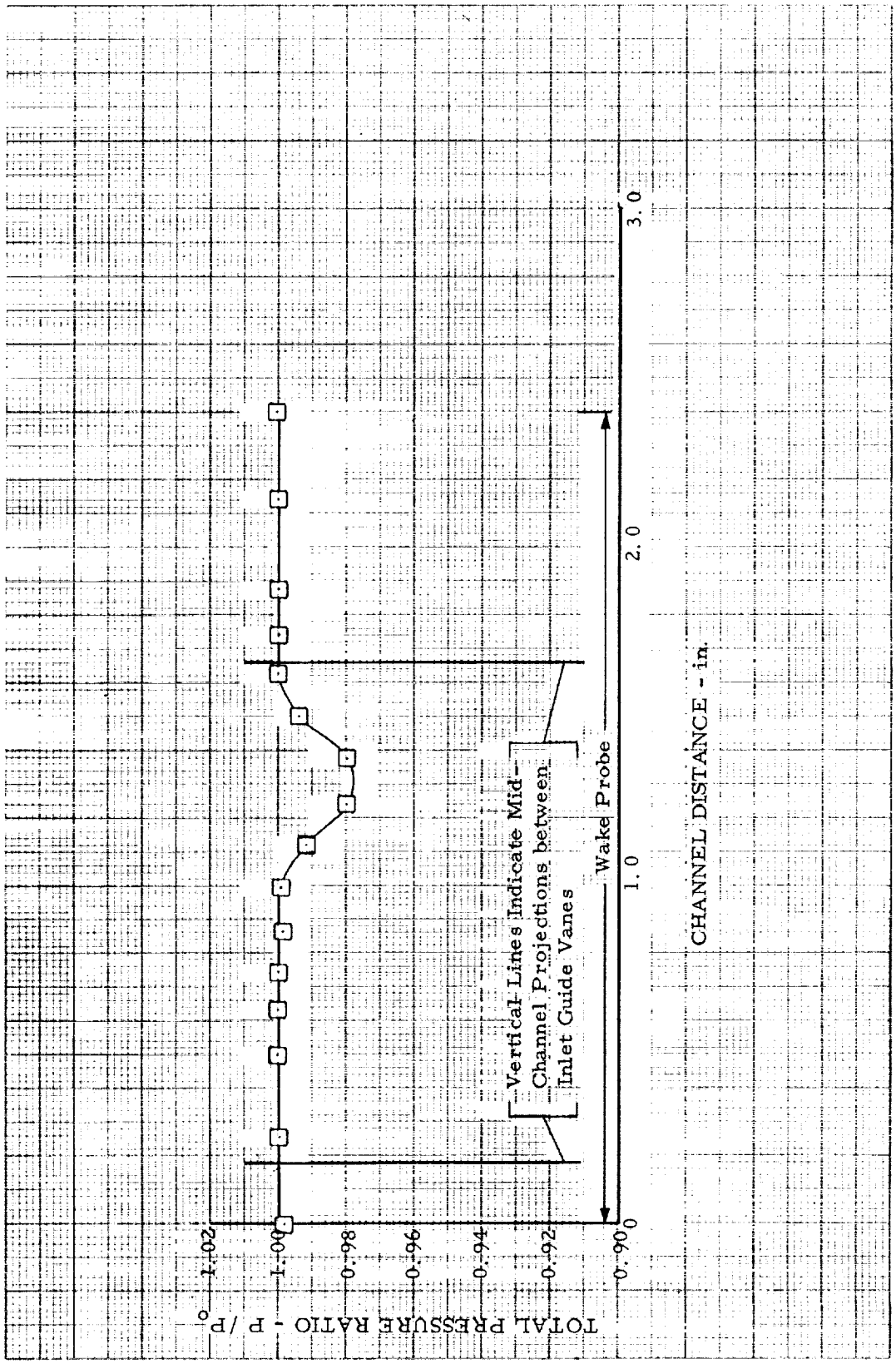

DF 45239

Figure V-2. Typical Inlet Guide Vane Wake Total Pressure Profile

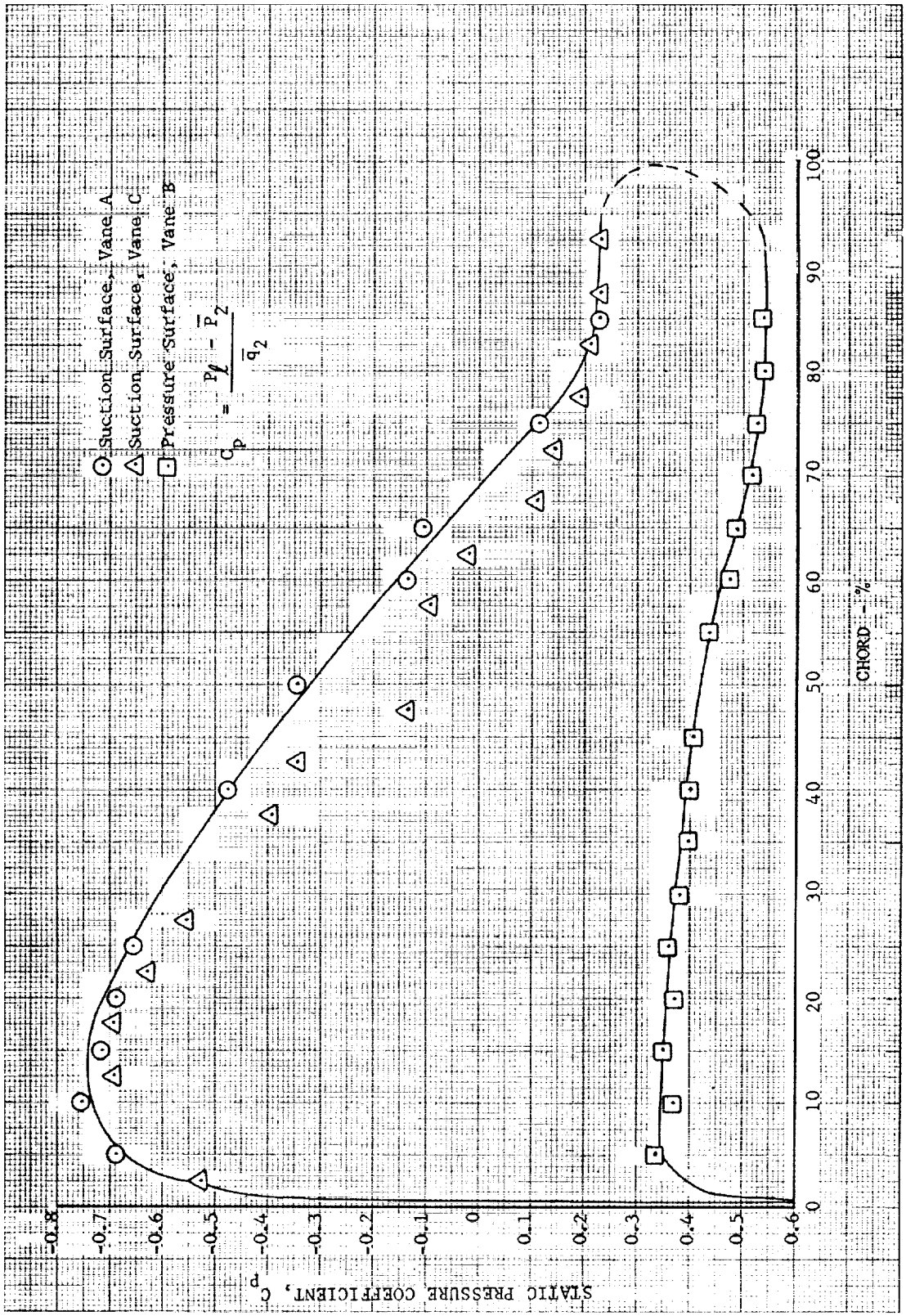

DF 49844

Figure V-3. Variation of Static Pressure Coefficient for Unslotted Stator Vane

Configuration 1
Vane A
Dye Injected through Pressure Tap No. 12

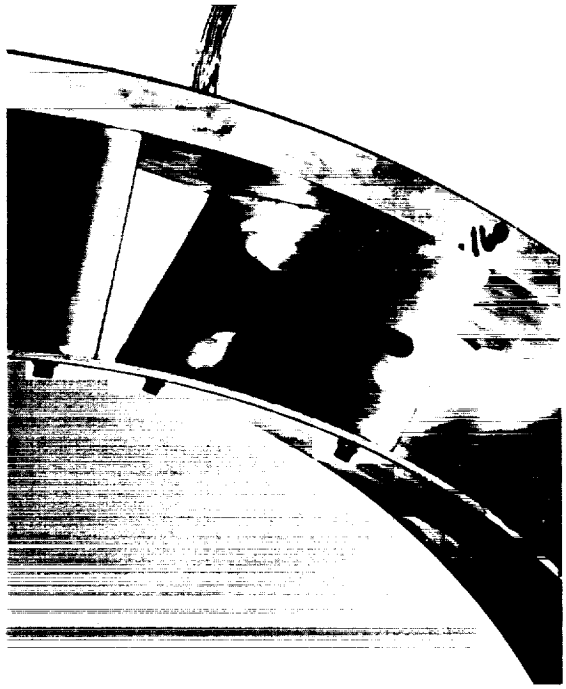

Configuration 1
Vane C
Dye Injected through Pressure Tap No. 21

Configuration 1A
Vane C
Dye Injected through Pressure Tap No. 31

Figure V-4. Dye Injection Pattern, Unslotted Configuration FD 15001A

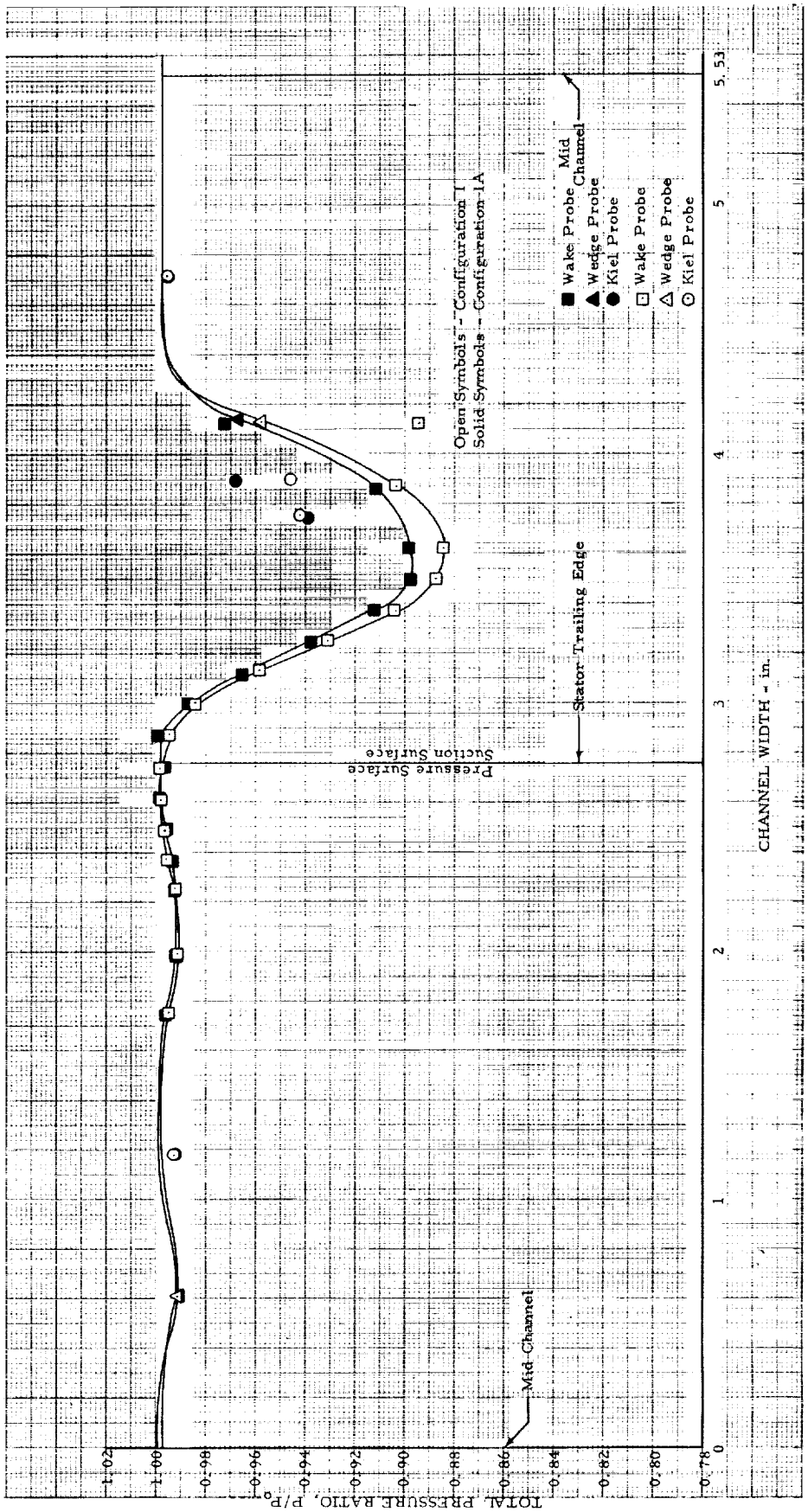

Figure V-5. Unslotted Stator Wake Total Pressure Profile

DF 49845

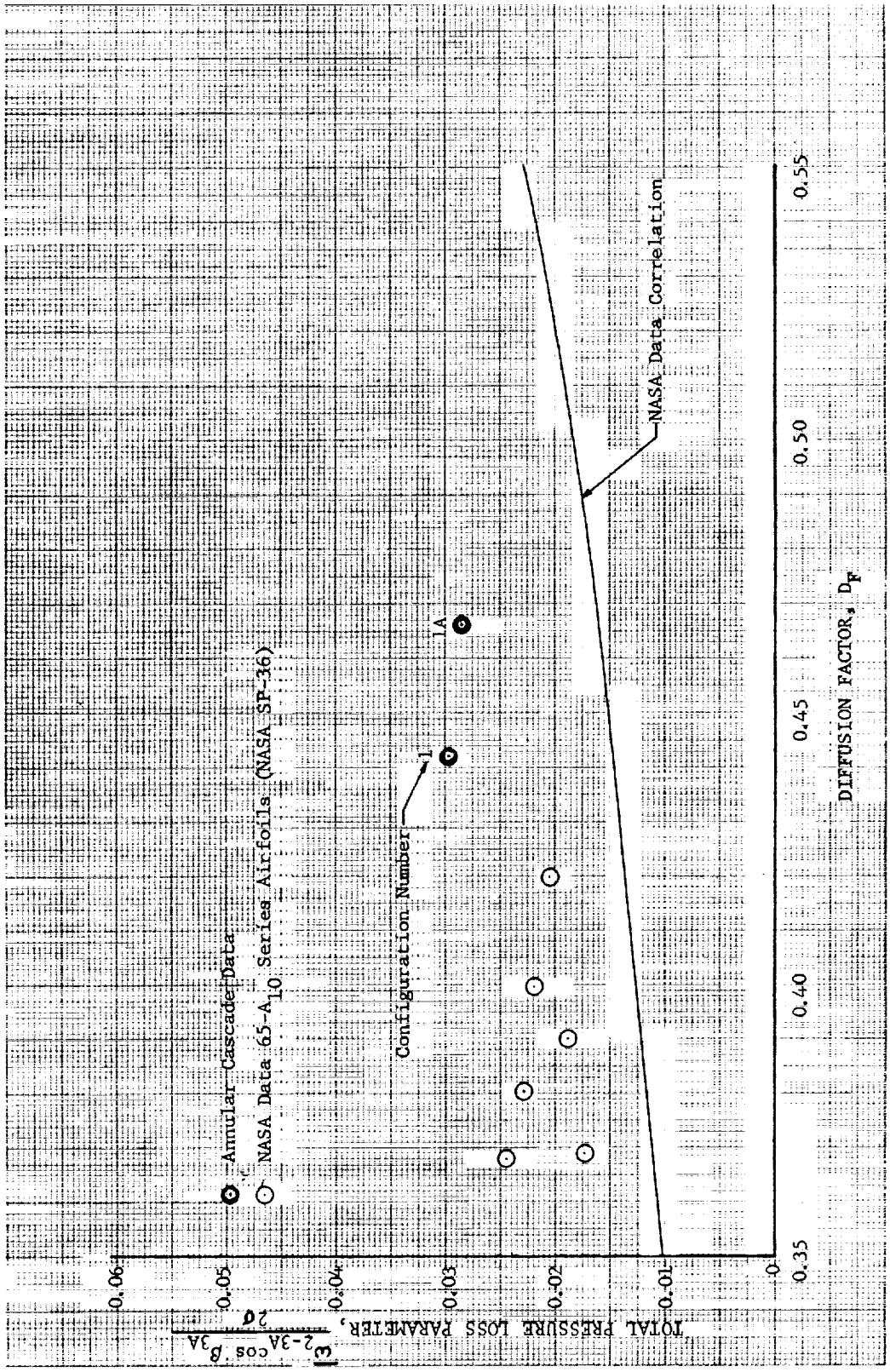

Figure V-6. Variation of Total Pressure Loss Parameter With Diffusion Factor (Unslotted Stators) DF 49846

R - Coanda Radius

r_1 - Slot Leading Edge Radius

Y_1 - Slot Capture Dimension

Y_2 - Slot Exit Dimension

ψ - Angle Formed by Slot Centerline and Mean Camber Line

Rp - Slot Pressure Surface Radius

Configuration	Y_2/Y_1	R, in.	r_1, in.	Y_1, in.	Y_2, in.	Slot Location
1	Unslotted					
2	0.770	0.458	0.028	0.182	0.140	Forward
4	0.770	0.280	0.028	0.182	0.140	Rear
5	0.600	0.458	0.028	0.233	0.140	Forward
6	0.770	0.535	0.028	0.182	0.140	Rear
7	0.450	0.458	0.028	0.311	0.140	Forward
8	0.680	0.535	0.028	0.206	0.140	Rear
9	0.486	0.458	0.056	0.288	0.140	Forward
10	0.710	Curve	0.028	0.206	0.146	Rear
14	0.590	Curve	0.036	0.254	0.150	Rear
15	0.291	0.458	0.056	0.244	0.070	Forward
18	0.435	Curve	0.056	0.244	0.106	Forward

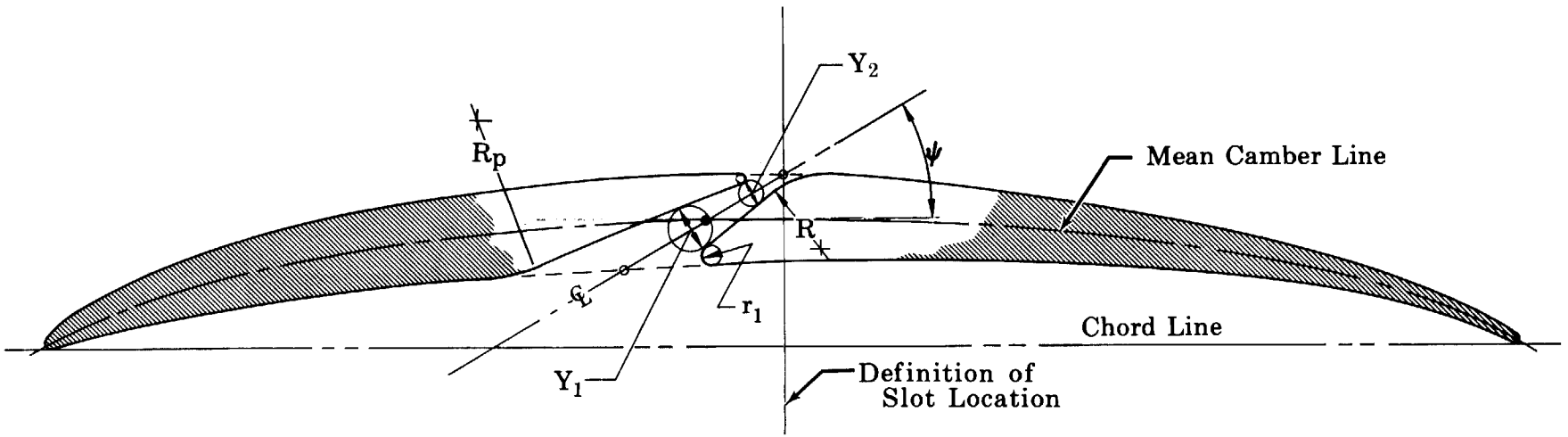

Figure V-7. Slot Geometry Nomenclature and Parameters

FD 14679C

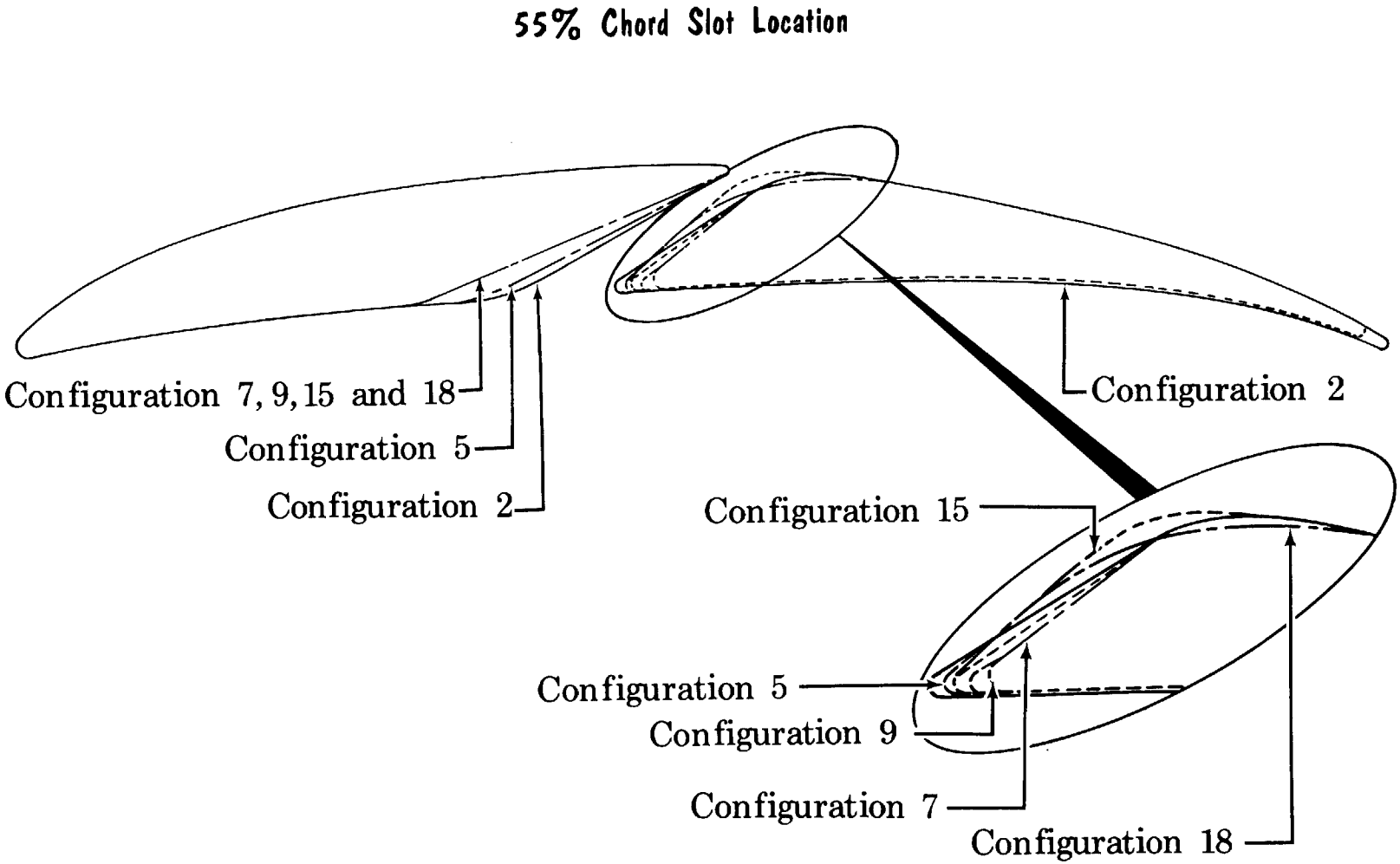

Figure V-8. Annular Cascade Stator Slot Configurations

FD 14678A

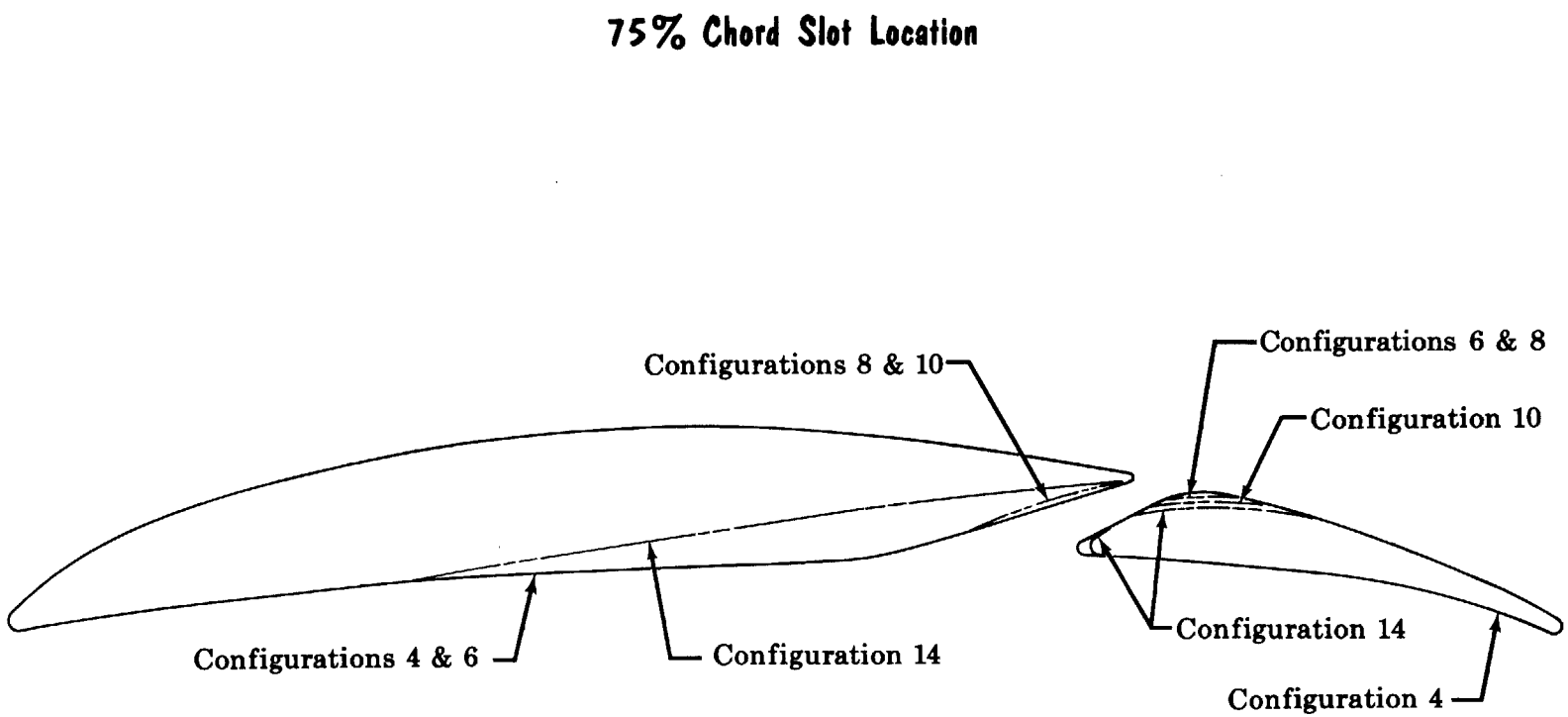

Figure V-9. Annular Cascade Stator Slot Configurations

FD 14677

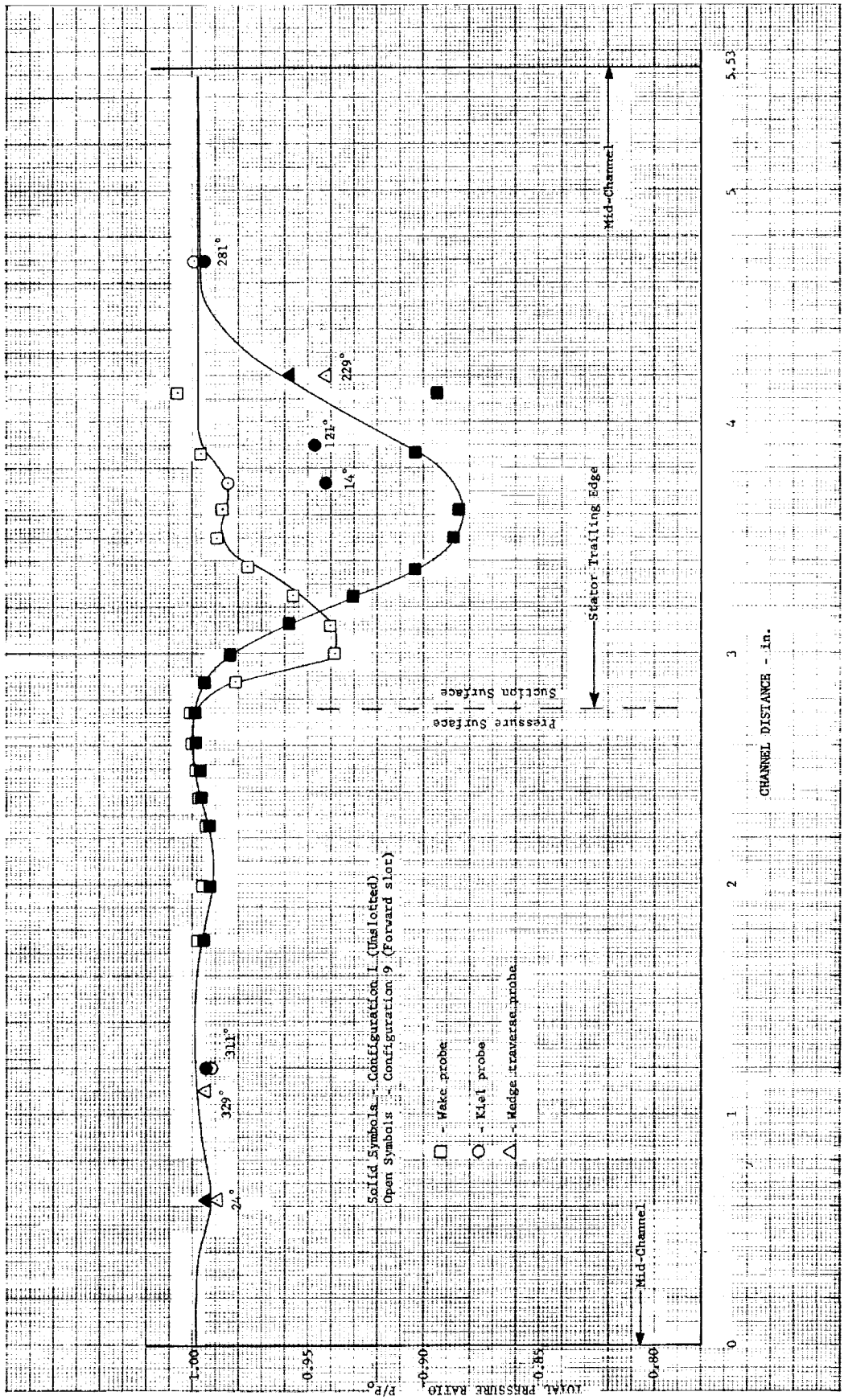

Figure V-10. Comparison Unslotted Stator Wake With Forward Slot Stator Wake

DF 45540

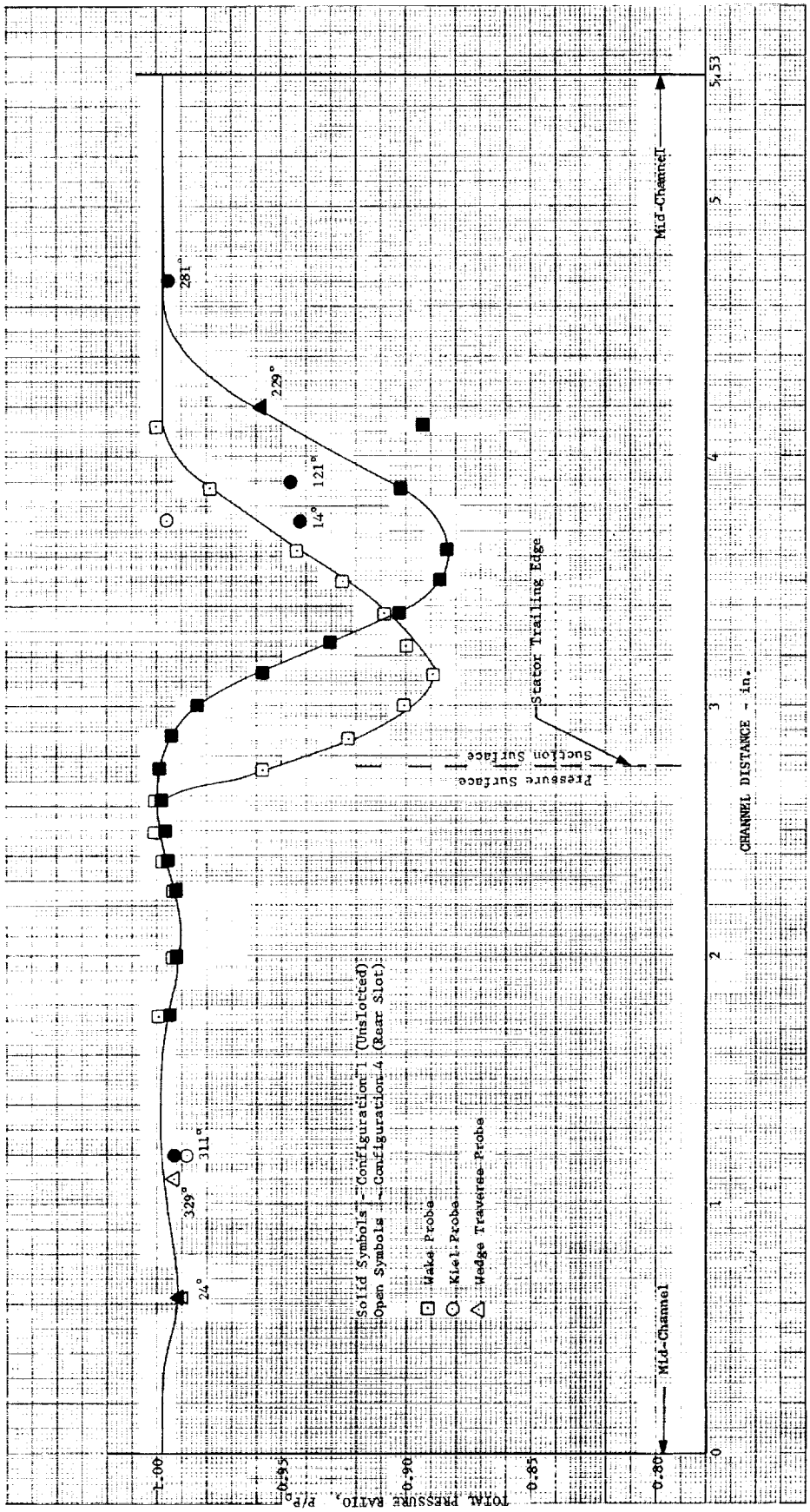

Figure V-11. Comparison of Unslotted Stator Wake With Rear Slot Stator Wake

DF 45541

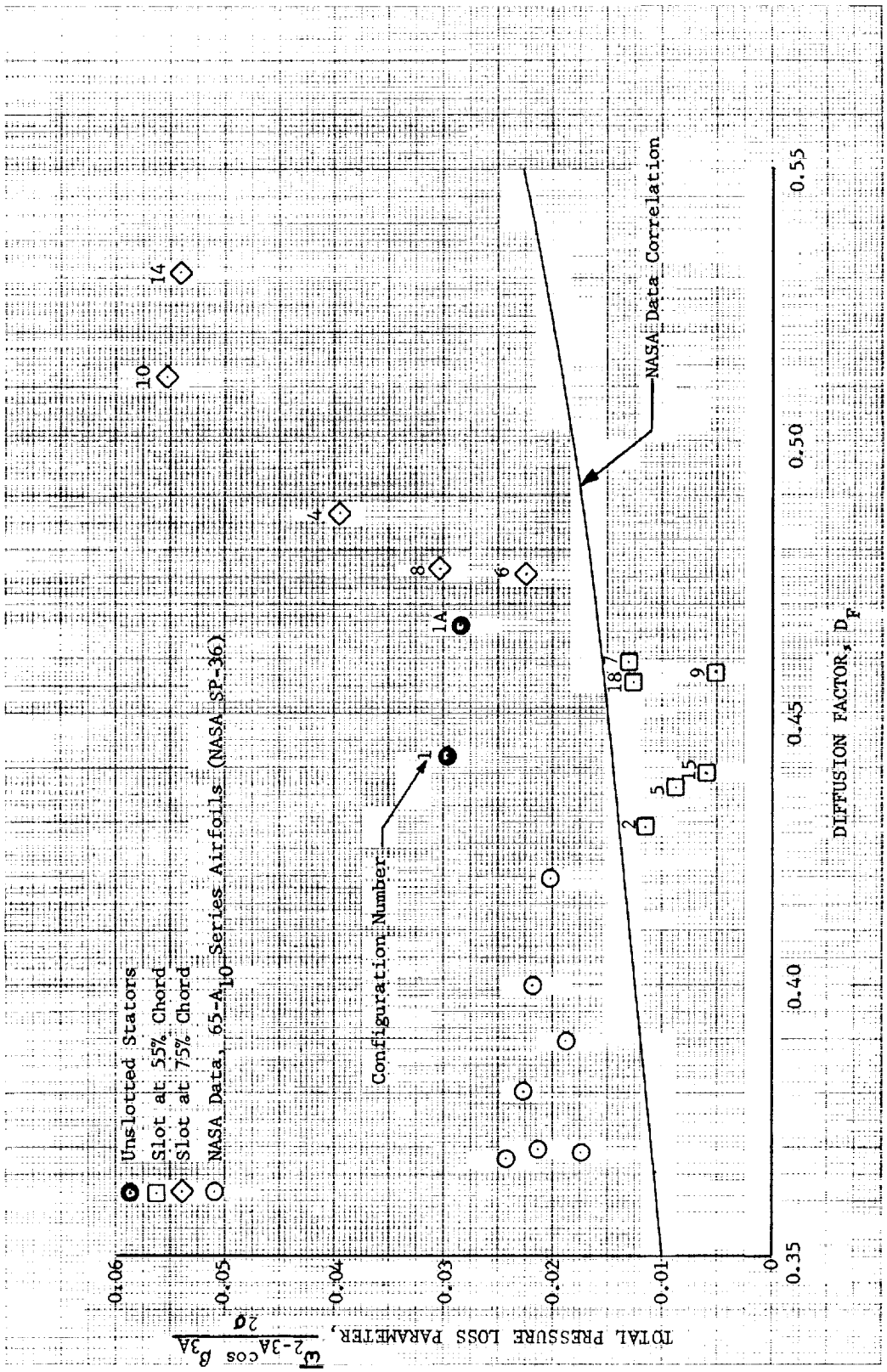

Figure V-12. Variation of Total Pressure Loss Parameter With Diffusion Factor (All Configurations) DF 49847

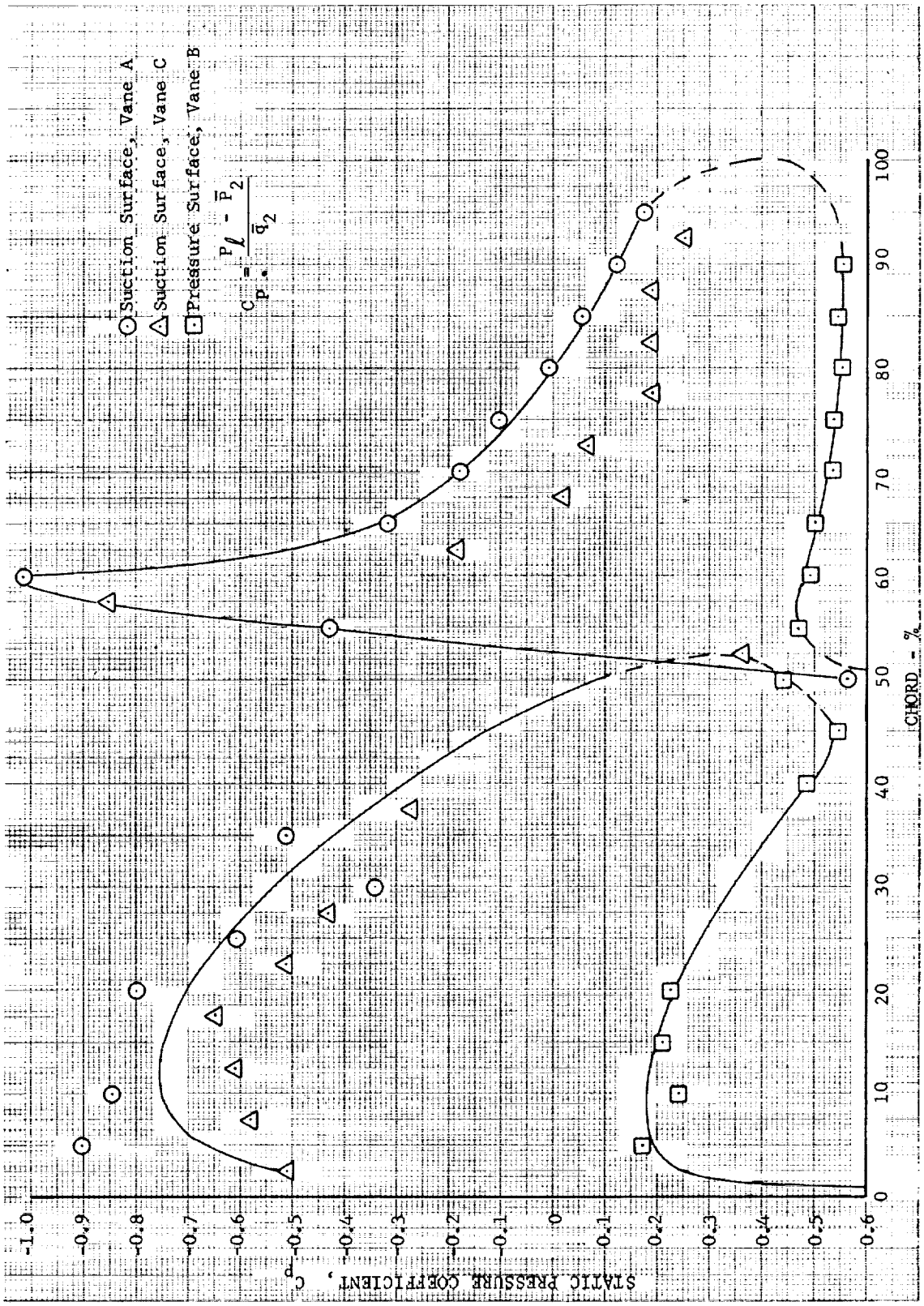

Figure V-13. Variation of Static Pressure Coefficient for Slotted Stator (Configuration 9) DF 49848

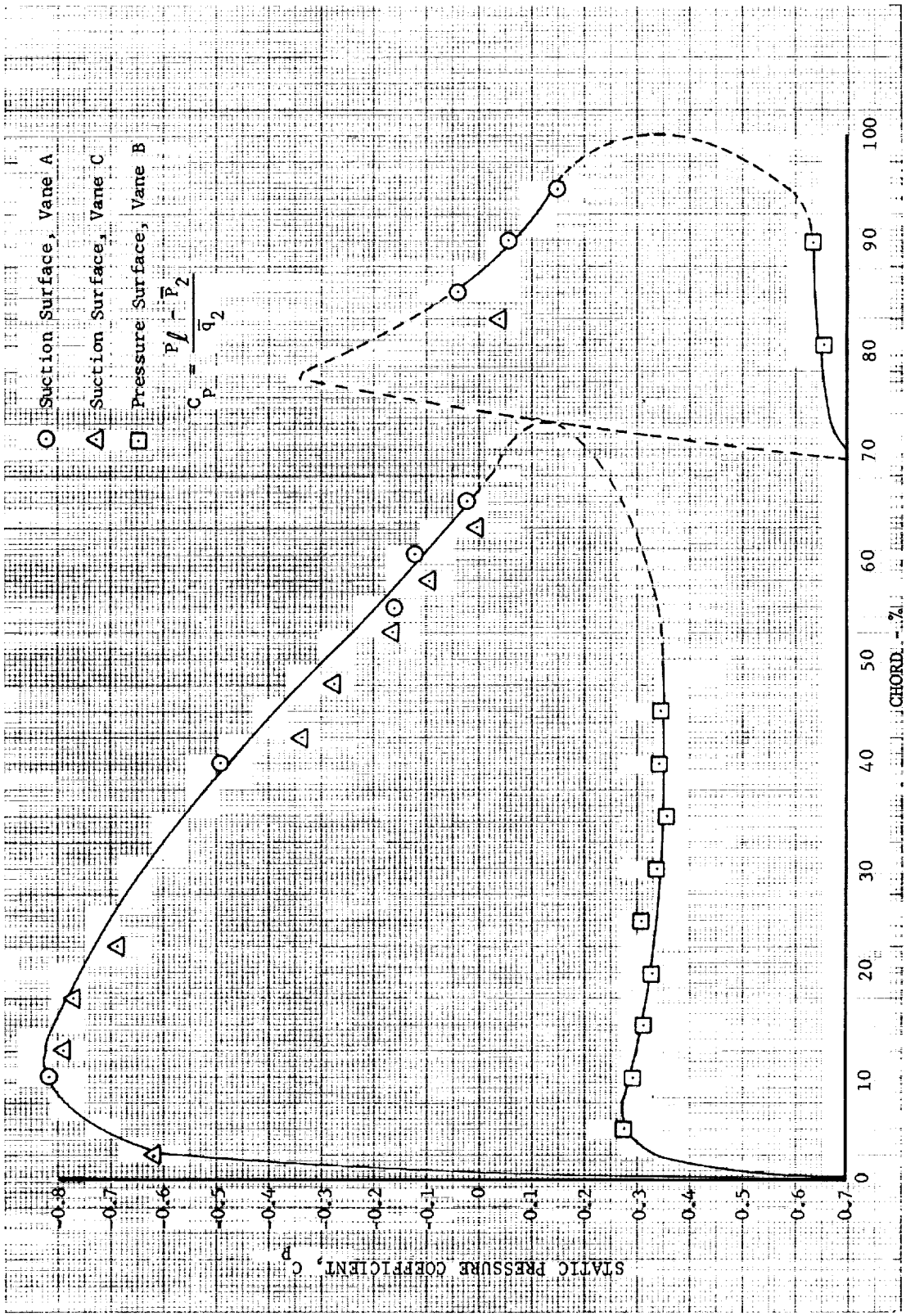

Figure V-14. Variation of Static Pressure Coefficient for Slotted Stator (Configuration 4) DF 49870

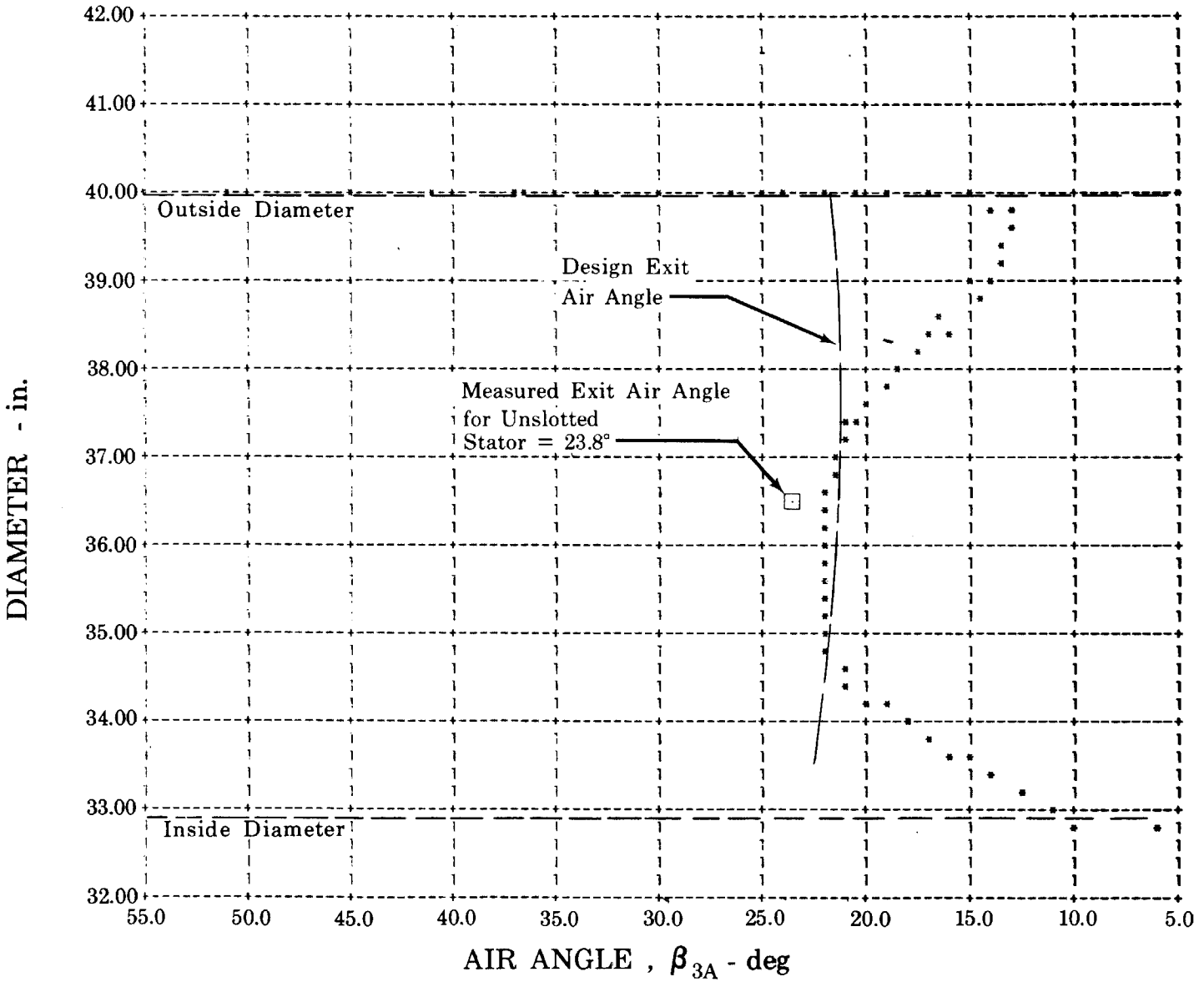

Figure V-15. IBM Plot of Stator Exit Air Angle Profile, Configuration 9, Station 3A FD 17443A